The University of Sydney

Department of Civil Engineering
Sydney NSW 2006
AUSTRALIA

http://www.civil.usyd.edu.au

Centre for Geotechnical Research

Research Report No R814

A Structured Cam Clay Model

By

Martin D Liu BE MPhil PhD
John P Carter BE PhD FIEAust MASCE

March 2002

The University of Sydney

Department of Civil Engineering
Centre for Geotechnical Research
http://www.civil.usyd.edu.au/

A Structured Cam Clay Model

Research Report No R814

Martin D Liu, BE, MPhil, PhD
John P Carter, BE, PhD, FIEAust, MASCE

ABSTRACT

A theoretical study of the behaviour of structured soil is presented. A new model, which is referred to as the Structured Cam Clay model, is formulated by introducing the influence of soil structure into Modified Cam Clay. The proposed model is hierarchical, *i.e.*, it is identical to the Modified Cam Clay soil model if a soil has no structure or if its structure is removed by loading. Three new parameters describing the effects of soil structure are introduced and the results of a parametric study are also presented. The proposed model has been used to predict the behaviour of structured soils in both compression and shearing tests. By making comparisons of predictions with experimental data and by conducting the parametric study it is demonstrated that the new model provides satisfactory qualitative and quantitative modelling of many important features of the behaviour of structured soils.

Keywords:
calcareous soils, clays, fabric, structure, constitutive relations, plasticity.

Copyright Notice

Department of Civil Engineering, Research Report R814
A Structured Cam Clay Model

m.liu@civil.usyd.edu.au; j.carter@civil.usyd.edu.au

Published by:
Department of Civil Engineering
The University of Sydney
Sydney NSW 2006
AUSTRALIA

March 2002

http://www.civil.usyd.edu.au

Contents

1. Introduction

Soils in situ usually possess natural structure, which enables them to behave differently from the same material in a reconstituted state (e.g., Burland, 1990; Leroueil and Vaughan, 1990; Cuccovillo and Coop; 1999). Recently, there have been important developments in formulating constitutive models incorporating the influence of soil structure, such as those proposed by Gens and Nova (1993), Whittle (1993), Wheeler (1997), Rouainia and Muir Wood (2000), and Kavvadas and Amorosi (2000). In this paper a new constitutive model for structured clays is proposed. The main objective of this new formulation is to provide a constitutive model suitable for the solution of boundary value problems encountered in geotechnical engineering practice. It is intended therefore, that the new model should be relatively simple and should have few parameters, each of which has a clear physical meaning and can be conveniently identified. The model should also be relatively easy to understand and apply.

The Modified Cam Clay model (Roscoe and Burland, 1968) is widely referenced and has been widely used in solving boundary value problems in geotechnical engineering practice (*e.g.*, Gens and Potts, 1988; Yu, 1998; Potts and Zdravkovic, 1999), although it was developed originally for reconstituted clays. Because of some familiarity with the model by the geotechnical profession and because it captures well the essential behaviour of reconstituted soil, the Modified Cam Clay model was chosen as the basis for the current research. A new model has been formulated by introducing the influence of soil structure into Modified Cam Clay. A parametric study demonstrating the capabilities and limitations of this new model is presented. The model has also been used to predict the behaviour of a variety of structured natural soils in both compression and shearing tests, allowing a reasonably comprehensive evaluation of it to be undertaken. It is demonstrated that the proposed new

model is suitable for describing the behaviour of a variety of natural clays and cemented soils.

2. Generalisation of Modified Cam Clay

The Modified Cam Clay model was proposed by Roscoe and Burland (1968) and a description and systematic study of the model can be found in the text by Muir Wood (1990). Formulations of this model suitable for use in finite element analysis can also be found in various texts (*e.g.*, Britto and Gun, 1987; Potts and Zdravkovic, 1999). In this paper, the Modified Cam Clay model is employed as a basis for formulating a hierarchical model for structured clays, which is referred to as the "Structured Cam Clay" model.

It is assumed that the behaviour of soil in a reconstituted state can be described adequately by the Modified Cam Clay model. The term "soil structure" is used here to mean the arrangement and bonding of the soil constituents, and for simplicity it encompasses all features of a soil that are different from those of the corresponding reconstituted soil. Following the suggestion of Burland (1990), the properties of a reconstituted soil are called the intrinsic properties, and are denoted by the symbol * attached to the relevant mathematical symbols. Hence, under all stress conditions, the influence of soil structure can be measured by comparing its behaviour with the intrinsic behaviour.

The formation and development of soil structure often produces anisotropy in the mechanical response of soil to changes in stress. Destructuring usually leads to the reduction of anisotropy. In order to concentrate on introducing the physical concepts of the framework and to avoid unnecessary complexity of mathematical detail, only the isotropic effects of soil structure are included in the proposed theoretical framework. The extension required to include the influence of soil anisotropy shall be a future research topic, however it is noted that others have previously considered this feature of soil behaviour, *e.g.*, Dafalias (1987), Whittle and Kavvadas (1994), Wheeler (1997) and Rouainia

and Muir Wood (2000). It should also be noted that coaxiality between the principal axes of plastic strain increment and those of stress is assumed in the proposed framework.

The stress and strain quantities used in the present formulation are defined as follows. σ'_{ij} and ε_{ij} are the cartesian components of effective stress and of strain respectively. The simplified forms for stress and strain conditions in conventional triaxial tests are also listed, where σ'_1 (or ε_1) and σ'_3 (or ε_3) are the axial effective stress (strain), and the radial effective stress (strain) respectively.

The mean effective stress p', deviatoric stress q and stress ratio η are given by

$$\begin{aligned} p' &= \frac{1}{3}(\sigma'_{11} + \sigma'_{22} + \sigma'_{33}) \\ &= \frac{1}{3}(\sigma'_1 + 2\sigma'_3) \text{ for conventional triaxial tests,} \end{aligned} \tag{1}$$

$$\begin{aligned} q &= \frac{1}{\sqrt{2}}\sqrt{\left[(\sigma'_{11} - \sigma'_{22})^2 + (\sigma'_{22} - \sigma'_{33})^2 + (\sigma'_{33} - \sigma'_{11})^2 + 6(\sigma'^{\,2}_{12} + \sigma'^{\,2}_{23} + \sigma'^{\,2}_{31})\right]} \\ &= (\sigma'_1 - \sigma'_3) \quad \text{for conventional triaxial tests,} \end{aligned} \tag{2}$$

$$\eta = \frac{q}{p'} \ . \tag{3}$$

The corresponding (work-conjugate) volumetric strain increment, $d\varepsilon_{v,}$, and deviatoric strain increment, $d\varepsilon_d$, are defined by

$$\begin{aligned} d\varepsilon_v &= d\varepsilon_{11} + d\varepsilon_{22} + d\varepsilon_{33} \\ &= d\varepsilon_1 + 2d\varepsilon_3 \text{ for conventional triaxial tests} \end{aligned} \tag{4}$$

and

$$d\varepsilon_d = \frac{\sqrt{2}}{3}\sqrt{\left[(d\varepsilon_{11}-d\varepsilon_{22})^2+(d\varepsilon_{22}-d\varepsilon_{33})^2+(d\varepsilon_{33}-d\varepsilon_{11})^2+6(d\varepsilon_{12}{}^2+d\varepsilon_{23}{}^2+d\varepsilon_{31}{}^2)\right]}$$
$$= \frac{2}{3}(d\varepsilon_1 - d\varepsilon_3) \quad \text{for conventional triaxial tests} \tag{5}$$

2.1 Influence of soil structure on virgin isotropic compression

The work by Liu and Carter (1999 and 2000) is employed here as a starting point for including the effects of soil structure in the model. The material idealisation of the isotropic compression behaviour of structured clay is illustrated in Fig. 1. In this figure e represents the voids ratio for a structured clay, e^* is the voids ratio for the corresponding reconstituted soil at the same stress state during virgin yielding, $p'_{y,i}$ is the mean effective stress at which virgin yielding of the structured soil begins, and Δe, the additional voids ratio, is the difference in voids ratio between a structured soil and the corresponding reconstituted soil at the same stress state. Hence, the virgin isotropic compression behaviour of a structured soil can be expressed by the following equation,

$$e = e^* + \Delta e \ . \tag{6}$$

The following equation was proposed by Liu and Carter (2000) to describe the volumetric behaviour of natural clays during virgin isotropic compression,

$$e = e^* + \Delta e_i \left(\frac{p'_{y,i}}{p'} \right)^b \ . \tag{7}$$

Δe_i is the additional voids ratio at $p' = p'_{y,i}$, where virgin yielding of the structured soil begins (Fig. 1). b is a parameter quantifying the rate of destructuring and it is referred to here as the *destructuring index*. The value of b depends on soil type and structure and generally $b \geq 1$ for soft structured clays and $b < 1$ for stiff clays. For the thirty different clays studied by Liu and Carter

(1999, 2000), it was found that generally $0 \le b \le 30$. For clay samples of a given mineralogy and with similar geological stress history but different depths below the surface, it is found that b depends mainly on the liquidity index.

2.2 Yield surface for structured clay

In the Modified Cam Clay model, the behaviour of a clay is divided into virgin yielding behaviour and elastic behaviour by its current elliptical yield surface. The size of the yield surface can be identified uniquely according to the stress state and the voids ratio and is a function of stress history. In the proposed Structured Cam Clay model, the behaviour of clay is also divided into virgin yielding behaviour and elastic behaviour by its current yield surface, which is dependent on soil structure as well as stress history. Hence, the current yield surface of a structured clay, named as the structural yield surface, is defined by its current stress state, voids ratio, stress history, and soil structure. Similar to the original proposal by Roscoe and Burland (1968), the yield surface of a structured soil in p'-q space is assumed to be elliptical in shape and it passes through the origin of the stress coordinates (Fig. 2). The aspect ratio for the structural yield surface is M*, the critical state strength of the reconstituted soil. One axis of the ellipse coincides with the p' axis. p'_s, the value of the p' coordinate where the ellipse again intersects the axis, represents the size of the yield surface. The yield surface is thus given by the yield function f, where

$$f = \left(\frac{q}{0.5\mathrm{M}^* p'_s} \right)^2 + \left(\frac{p' - 0.5 p'_s}{0.5 p'_s} \right)^2 - 1 = 0 \quad . \tag{8}$$

2.3 Volumetric deformation for virgin yielding along general stress paths

As illustrated in Fig. 1, virgin yielding and elastic behaviour of reconstituted clay, *i.e.*, a clay where structure is completely removed, are both linear in e - $\ln p'$ space, with gradients λ^* and κ^* respectively. The isotropic virgin compression line for the reconstituted soil, *i.e.*, ICL*, is given by

$$e^* = e^*_{IC} - \lambda^* \ln p' \tag{9}$$

where e^*_{IC} is the voids ratio of the reconstituted soil when p' = 1 kPa during virgin isotropic compression. We seek now to generalise equation (9) for a soil that possesses structure.

Consider loading where the current stress state stays on the yield surface, and the size of the current yield surface is denoted as p'_s. For monotonic loading, virgin yielding occurs if $p'_s \geq p'_{y,i}$.

Under the assumption that the hardening of structured soil is dependent on the plastic volumetric deformation, the yield surface for a structured soil is defined by all stress states that have the same accumulation of absolute plastic volumetric strain. In such a model the plastic volumetric deformation is dependent on the change in size of the yield surface only. If the elastic deformation for a structured soil is assumed to be the same as that of the reconstituted soil, any change in the additional voids ratio sustained by soil structure must also be associated with plastic volumetric deformation, and therefore is also dependent on the size of the yield surface. Consequently, the variable p' in formula (7) may be written in terms of the size of the current yield surface p'_s. On substituting equation (9) into equation (7), the following expression for the variation of the voids ratio is obtained

$$e = e^*_{IC} + \Delta e_i \left(\frac{p'_{y,i}}{p'_s} \right)^b - \lambda^* \ln p' \text{ for } p'_s \geq p'_{y,i} \ . \tag{10}$$

$p'_{y,i}$ is the value of the mean effective stress at the initial yield point for an isotropic stress state, and is numerically equal to the size of the initial yield surface associated with the initial soil structure.

According to Critical State Soil Mechanics (Schofield and Wroth, 1968), for compression along a general stress path the volumetric deformation defined by

$\lambda^*\ln p'$, which is associated with intrinsic soil properties, can be divided into two parts. The elastic part is defined by $\kappa^*\ln p'$, which is dependent on the current mean effective stress, and the plastic part is given by $(\lambda^*-\kappa^*)\ln p_s'$, which is dependent on the size of the yield surface. The voids ratio for a structured soil during virgin compression along a general stress path is thus obtained as follows:

$$e = e^*_{IC} + \Delta e_i \left(\frac{p'_{y,i}}{p'_s} \right)^b - (\lambda^* - \kappa^*) \ln p'_s - \kappa^* \ln p' \ . \tag{11}$$

The general compression equation (11) states that voids ratio for a structured soil during virgin compression is dependent on two parts, *viz.* the elastic part which is dependent on the current mean effective stress, and the plastic part which is dependent on the size of the current yield surface. The plastic part is again subdivided into two parts, *viz.* the part associated with the intrinsic properties of the soil and that associated with soil structure.

Differentiating equation (11) and noting equations (6) and (7), the total volumetric strain increment for compression along a general stress path is obtained as follows

$$d\varepsilon_v = (\lambda^* - \kappa^*) \frac{dp'_s}{(1+e)p'_s} + b\Delta e \frac{dp'_s}{(1+e)p'_s} + \kappa^* \frac{dp'}{(1+e)p'} \ . \tag{12}$$

The last part of the expression for the total volumetric strain, *i.e.*, the last term on the right hand side of equation (12), is associated with elastic deformation. Hence

$$d\varepsilon_v^e = \kappa^* \frac{dp'}{(1+e)p'} \tag{13}$$

and

$$d\varepsilon_v^p = (\lambda^* - \kappa^*)\frac{dp'_s}{(1+e)p'_s} + b\Delta e\frac{dp'_s}{(1+e)p'_s} \quad . \tag{14}$$

The plastic volumetric strain is therefore made up of two parts. The first part is dependent on the intrinsic soil properties and has been described already by the Modified Cam Clay model. The second part is dependent on soil structure and is responsible for the reduction of the additional voids ratio sustained by soil structure. Hence, this part represents the effect of structure and destructuring. It may be seen from equation (14) as well as equation (11) that the plastic volumetric deformation associated with destructuring is also dependent on the change in size of the yield surface, irrespective of the magnitude of the current shear stress. Considering the mechanism of shearing, it is rational to assume that destructuring and the associated plastic volumetric deformation should be dependent on both the change in size of the yield surface and the magnitude of the current shear stress. Therefore, a modification of equation (14) is made so that the effect of shear stress on destructuring is also considered, *i.e.*,

$$d\varepsilon_v^p = (\lambda^* - \kappa^*)\frac{dp'_s}{(1+e)p'_s} + b\Delta e\left(1 + \frac{\eta}{\mathrm{M}^* - \eta}\right)\frac{dp'_s}{(1+e)p'_s} \tag{15}$$

where η is the shear stress ratio defined in equation (3). It may be seen from equation (15) that the effect of destructuring, which is described as the reduction of the additional voids ratio, increases with the value of the current stress ratio.

Alternatively, equation (15) can be rewritten as

$$d\varepsilon_v^p = (\lambda^* - \kappa^*)\frac{dp'_s}{(1+e)p'_s} + b\Delta e\left(\frac{\mathrm{M}^*}{\mathrm{M}^* - \eta}\right)\frac{dp'_s}{(1+e)p'_s} \quad . \tag{16}$$

Because of the modification made to equation (12), the new hardening rule for a structured soil is no longer dependent only on the plastic volumetric deformation. It also depends on the shear stress ratio, η.

In summary, structured clay is idealised here as an isotropic hardening and destructuring material with elastic and virgin yielding behaviour. It is assumed that during virgin yielding the yield surface includes the current stress state and expands isotropically causing destructuring of the material.

2.4 Flow rule

In the Modified Cam Clay model, associated plastic flow is assumed. Thus, the yield surface is also the plastic potential and the flow rule is given as

$$\frac{d\varepsilon_d^p}{d\varepsilon_v^p} = \frac{2\eta}{\mathrm{M}^{*2} - \eta^2} \quad . \tag{17}$$

The structure of soil also has influence on the flow rule. It is observed that a structured clay with positive Δe generally has a lower value for the strain increment ratio $d\varepsilon^p_d/d\varepsilon^p_v$ than the corresponding reconstituted soil at the same virgin yielding stress state (*e.g.*, Olson, 1962; Graham and Li, 1985; Cotecchia and Chandler, 1997). The following equation is therefore proposed as a flow rule for structured clay,

$$\frac{d\varepsilon_d^p}{d\varepsilon_v^p} = \frac{2(1-\omega\Delta e)\eta}{\mathrm{M}^{*2} - \eta^2} \quad . \tag{18}$$

ω is a new model parameter which describes the influence of soil structure on the flow rule. The modifier should not be negative otherwise the plastic strain increment vector will always be directed inside the yield surface. Hence, based on the need to meet this condition at all times, including the start of virgin yielding, the following constraint is imposed:

$$0 < 1 - \omega\Delta e_i \leq 1 \tag{19}$$

and therefore

$$0 \leq \omega \leq \frac{1}{\Delta e_i} \quad . \tag{20}$$

Equation (18) implies a non-associated plastic flow rule for the new model. This feature has important consequences for numerical solution schemes employing the model to solve boundary value problems. In particular, it generally results in the governing equations being non-symmetric.

2.5 Additional assumptions

For the proposed new model the following additional assumptions are made.

(1) The behaviour of structured soil is divided into an elastic region and a virgin yielding region by the current yield surface.

(2) During virgin yielding the yield surface expands isotropically and includes the current stress state.

Consequently, the initial yield surface, denoted as $p'_{y,i}$, is the current yield surface for any stress excursion inside the initial yield surface. The current yield surface is defined as the maximum yield surface the soil has ever experienced if the stress state of the soil has exceeded the initial yield surface. Therefore, the current yield surface in the proposed model is assumed as the maximum yield surface encountered by the soil, and the minimum value of p'_s is numerically equal to $p'_{y,i}$.

(3) The effect of anisotropy on soil deformation is not considered.

In this model, structured clay is idealised as an isotropic hardening and destructuring material with elastic and virgin yielding behaviour. The influence of soil anisotropy is not considered in this paper in order to provide a relatively simple model within the well-known Cam Clay framework. Modelling the anisotropic properties of soils can be found in works such as those reported by Dafalias (1987), Whittle and Kavvada (1994), Wheeler (1997) and Rouainia and Muir Wood (2000).

3. Stress-Strain Relationships

3.1 Elastic deformation

For stress excursions within the current yield surface, only elastic deformation occurs. The elastic deformation of a structured soil is assumed to be independent of soil structure. According to the Modified Cam Clay model, the elastic strain increment can be expressed as

$$d\varepsilon_v^e = \left(\frac{\kappa^*}{1+e}\right)\frac{dp'}{p'} \tag{21}$$

$$d\varepsilon_d^e = \frac{2(1+\nu^*)}{9(1-2\nu^*)}\left(\frac{\kappa^*}{1+e}\right)\frac{dq}{p'} \tag{22}$$

where ν* is Poisson's ratio. The assumption of a constant Poisson's ratio leads to a non-conservative response to cyclic loading, but is a common feature of the Cam clay models.

3.2 Virgin yielding

For stress states on the yield surface and with $dp'_s > 0$, virgin yielding occurs. Based on the plastic volumetric deformation, *i.e.*, equation (16), the flow rule given by equation (18) and considering the elastic deformation, the following stress and strain relationships for virgin yielding are obtained

$$d\varepsilon_v = \kappa^*\frac{dp'}{(1+e)p'} + (\lambda^*-\kappa^*)\frac{dp'_s}{(1+e)p'_s} + b\Delta e\left(\frac{\mathrm{M}^*}{\mathrm{M}^*-\eta}\right)\frac{dp'_s}{(1+e)p'_s}\ , \tag{23}$$

$$d\varepsilon_d = \frac{2(1+\nu^*)}{9(1-2\nu^*)}\left(\frac{\kappa^*}{1+e}\right)\frac{dq}{p'} + \frac{2\eta(1-\omega\Delta e)}{(\mathrm{M}^{*2}-\eta^2)}\left[(\lambda^*-\kappa^*)+b\Delta e\left(\frac{\mathrm{M}^*}{\mathrm{M}^*-\eta}\right)\right]\frac{dp'_s}{(1+e)p'_s}\ . \tag{24}$$

3.3 Softening

Soil is regarded as an elastic material for loading inside the virgin yield surface. When the current stress state reaches the virgin yield surface at a point with

$dp'_s > 0$ virgin yielding occurs. If the soil reaches the yield surface with $\eta > \mathrm{M}^*$, softening occurs if the boundary conditions allow appropriate adjustment of the stress state. Otherwise, catastrophic failure will be predicted. During the softening process, soil structure will be broken down, and the yield surface shrinks with the current stress state always remaining on it. In such cases the yield surface contracts until the soil reaches a critical state of deformation where the structure of the soil is completely removed. It follows, therefore, that the softening behaviour of a soil should be described by virgin yielding equations. Consequently, the plastic volumetric strain increment given by equation (16) should also be valid for the softening process. It may be noticed that because the yield surface shrinks the volumetric deformation associated with intrinsic soil properties is negative, *i.e.*, expansive. However, the volumetric deformation associated with the destructuring is determined by Δe, because both the terms (M^*-η) and dp'_s are negative. If Δe is positive, this part of the overall volumetric deformation is positive. If Δe is negative, the structural part of the volumetric deformation is negative. This is rational because destructuring occurs during the softening process, and consequently the additional voids ratio sustained by soil structure necessarily decreases. As a result, softening of structured clays can be accompanied by either overall volumetric expansion (negative pore pressure for undrained tests), or overall volumetric compression (positive pore pressure for undrained tests). This tendency can be seen in test data for both natural soils and artificially structured soils reported by several researchers, including Lo (1972), Nambiar *et al.* (1985), Burland *et al.* (1996), and Carter *et al.* (2000).

The plastic deviatoric strain increment during softening is proposed as follows,

$$d\varepsilon_d^p = 2(1-\omega\Delta e)\left[(\lambda^* - \kappa^*) - b\Delta e\left(\frac{\mathrm{M}^*}{\mathrm{M}^* - \eta}\right)\right]\frac{\eta}{(\mathrm{M}^{*2} - \eta^2)(1+e)p'_s}\frac{dp'_s}{} \quad . \qquad (25)$$

Compared with equation (24), it can be seen that only the sign of the plastic deviatoric strain associated with destructuring is changed, so that the strain increment vector will point outside the yield surface.

The elastic part of the deformation can be calculated by equations (21) and (22). The total strain increments during softening are thus fully determined. As softening is a strained-controlled process, the change in the stress state can be decided from the size of the current structural yield surface. When condition $\eta = M^*$ is reached, the structure of soil is usually completely destroyed with $\Delta e = 0$, and therefore, the structured clay has reached the critical state of deformation.

It may be noticed that for both virgin yielding and softening behaviour the soil may reach a state with $\eta = M^*$ but with $\Delta e \neq 0$. A specific example is the case where a soil reaches critical state by loading entirely inside the yield surface. In this case virgin yielding commences once the yield surface is reached and, according to equations (23) and (24), the soil is also in a state where it can be distorted continuously at constant volume ($d\varepsilon vp = 0$ and $d\varepsilon vp \rightarrow$). Hence, the proposed model predicts that under special stress paths a soil may reach a critical state of deformation with its structure having not been removed completely. Consequently, in such cases the soil state will not be on the critical state line defined in e - p′ space. If there is evidence that the structure of a soil is destroyed completely after the soil reaches the critical state of deformation then destructuring could be described by the plastic distortional strain instead of the current stress ratio. However, this possibility has not been pursued here.

4. Parameter Determination

Eight parameters define the proposed model, and they are M^*, e^*_{IC}, λ^*,κ^*, ν^*, b, $p'_{y,i}$, and ω. The first five parameters, denoted by the symbol *, are intrinsic soil properties and are independent of soil structure. These five intrinsic

parameters are the same as those adopted in the Modified Cam Clay model (Roscoe and Burland, 1968). The influence of these parameters will not be investigated in this paper since studies of them are well documented (*e.g.*, see Muir Wood, 1990).

Three new parameters, *viz.*, b, $p'_{y,i}$ and ω, are introduced to describe the influence of soil structure on its mechanical behaviour. The value of the destructuring index, b, indicates the rate of the destructuring during virgin yielding (Fig. 1), and $p'_{y,i}$ represents the size of the initial yield surface for a structured soil (Fig. 5). The values of these two parameters can be determined directly from an isotropic compression test on an intact (undisturbed) soil specimen. Parameter ω was introduced to describe the influence of soil structure on the flow rule (*e.g.*, see equation (18)), and its value can be determined by applying the flow rule to the strains measured in a shearing test on an intact specimen provided that the elastic properties of the soil are known.

Values of five of the model parameters, viz., e^*_{IC}, λ^*,κ^*, b, and $p'_{y,i}$ can be determined from isotropic compression tests. The values of parameters λ^* and κ^* and b can be determined directly from any compression tests with constant η, whereas the values of e^*_{IC} and $p'_{y,i}$ can only be determined directly from isotropic tests. In geotechnical engineering practice oedometer tests on soils are much more widespread than isotropic compression tests. Therefore approximate methods for obtaining soil parameters e^*_{IC} and $p'_{y,i}$ from oedometer tests, as well as any constant η tests, are also proposed.

The behaviour of reconstituted clay is assumed to follow the assumptions of Critical State Soil Mechanics (*e.g.*, details see Muir Wood, 1990). For a reconstituted soil with a given mineralogy, the compression lines with different stress ratio η are therefore assumed parallel (Fig. 4). The difference in voids ratio between e^*_{IC} and e^*_{η}, the voids ratio at $p' = 1$ kPa for a compression test with constant η, can therefore be expressed as

$$e^*_{IC} = e^*_{\eta} + (\lambda^* - \kappa^*)\ln\left(\frac{p'_o}{p'}\right). \tag{26}$$

The size of a yield surface p'_o and the mean effective stress for a stress state on the yield surface with stress ratio η are related as follows,

$$\frac{p'}{p'_o} = \frac{M^{*2}}{M^{*2} + \eta^2}. \tag{27}$$

Based on equations (26) and (27), the size of the initial yield surface $p'_{y,i}$ can be computed if the value of the mean effective stress at the virgin yield point is measured from a compression test with constant η, and the soil parameter e^*_{IC} can therefore be computed from the measured value of e^*_{η}.

For oedometer tests, an approximation is made based on Jacky's empirical equation (Jacky, 1944), in which the horizontal effective stress σ'_v and the vertical effective stress σ'_h for a soil during one dimensional virgin compression is expressed as

$$\frac{\sigma'_h}{\sigma'_v} \approx 1 - \sin\varphi_{cs} \tag{28}$$

where φ_{cs} is the critical state friction angle measured from a triaxial compression test. The critical state strength parameter M* can be expressed in terms of φ_{cs} as

$$M^* = \frac{6\sin\varphi_{cs}}{3 - \sin\varphi_{cs}}. \tag{29}$$

The relationship between σ'_v and p' for one-dimensional compression can be obtained as

$$\frac{\sigma'_v}{p'} = \frac{3}{3 - 2\sin\varphi_{cs}}. \tag{30}$$

Thus the stress ratio for a one-dimensional compression test can be expressed as

$$\eta = \frac{3\sin\varphi_{cs}}{3-2\sin\varphi_{cs}} \ . \tag{31}$$

Consequently, the following equation can be derived for estimating the size of the initial yield surface based on the initial vertical yield stress measured from an oedometer test,

$$p'_{y,i} = \left(1-\frac{2}{3}\sin\varphi_{cs}\right)\left[1+\left(\frac{3-\sin\varphi_{cs}}{6-4\sin\varphi_{cs}}\right)^2\right]\sigma'_{vy,i} \ . \tag{32}$$

e^*_{IC} can be related to the value of e^*_η obtained from an oedometer test by the following equation,

$$e^*_{IC} = e^*_\eta + (\lambda^* - \kappa^*)\ln\left\{\left(1-\frac{2}{3}\sin\varphi_{cs}\right)\left[1+\left(\frac{3-\sin\varphi_{cs}}{6-4\sin\varphi_{cs}}\right)^2\right]\right\} \ . \tag{33}$$

It should be pointed out that the proposed methods, based on the results of oedometer tests, are approximate and should be used only when more accurate methods for deriving the soil parameters are not available.

5. Features of the Model

The influence of the three new parameters b, $p'_{y,i}$ and ω, and some features of the new Structured Cam Clay model are described in this section. Example calculations have been made using the new model and the values of the intrinsic soil properties adopted are listed in Table 1. Based on these values, it is found that $e^*_{cs} = 2.1$, where e^*_{cs} is the well known parameter defining the position of the critical state line in $e - p'$ space.

Table 1 Model parameters

Parameter	M*	λ*	κ*	e^*_{IC}	ν*
Value	1.20	0.16	0.05	2.176	0.25

5.1 Parameter *b*

The influence of the destructuring index b is demonstrated by the simulations shown in Figs 5 and 6. The following values of parameters for the soil structure were employed in these calculations: $p'_{y,i} = 100$ kPa and $\omega = 1$. Eight different values of b were assumed and they are 0, 0.25, 0.5, 1, 2, 5, 10 and 100. The initial stress state was $p' = 100$ kPa and $q = 0$, and the initial value of the additional voids ratio was $\Delta e_i = 0.8$.

It can be seen that the destructuring index b has the following effects on the simulated isotropic compression behaviour (Fig. 5).

The compression behaviour of structured soil is asymptotic to that of the corresponding reconstituted soil for situations with $b > 0$.

The rate of reduction in the additional voids ratio maintained by soil structure increases with the magnitude of b. For situations with $b \geq 100$, there is almost an immediate collapse of soil structure when the initial yield stress is surpassed.

For $b = 0$, the virgin compression line for a structured soil and that for its corresponding reconstituted soil are parallel in the $e - \ln p'$ space. Theoretically, in this case no destructuring takes place during the virgin yielding and Δe remains unchanged.

The simulated shearing behaviour of a structured soil with different values of the destructuring index b is shown in Fig. 6. The effective stress paths

simulated follow those in a conventional drained triaxial test by increasing the axial loading only. The following features of soil behaviour are simulated.

Except for the unlikely situation with $b = 0$, the final state for a structured soil under monotonic shearing is independent of soil structure and is at the critical state of deformation. At this state the structure of soil has been completely removed. For the simulated cases where the initial stress state and voids ratio and the loading path are the exactly the same, the final states for all seven cases fall onto the same point on the critical state line (Fig 6a), and the final values of the deviatoric stress and the volumetric strain are the same (Figs 6b and 6c). Therefore parameter b has no influence on the final state of the soil under monotonic shearing if $b > 0$.

As has been discussed previously, there is no destructuring for the situation with $b = 0$. The final state of the soil does not fall onto the critical state line (Fig. 6a). The structure of the soil remains intact even when the soil is sheared to failure, *i.e.*, where the soil has no resistance to further distortional deformation. This particular situation is most likely a hypothetical limit state of the resistance of soil structure. Whether the structure of real geotechnical materials under extreme situations may respond to shearing in a manner similar to that described by $b = 0$ is probably unlikely but needs further investigation.

It can be seen from the stress path in the e-lnp' coordinates (Fig. 6a) that the rate of destructuring increases with the value of b. For the situation with $b = 100$ soil structure is destroyed almost immediately, where there is a sharp drop in voids ratio when shearing commences. After the structure of the soil has been removed, the reduction in the voids with loading is much slower and the behaviour of the original structured soil is the same as that of the corresponding reconstituted soil. This conclusion is confirmed by the deviatoric and volumetric strain relationship (Fig. 6b). The final volumetric strain for all the cases simulated is the same, however the deviatoric strain at which the soil reaches its final volumetric strain decreases with the increase of b.

For small strains, say $\varepsilon_d < 1\%$, the shear stiffness decreases with b. For relatively large deformation, to say with $\varepsilon_d > 1\%$, the shear stiffness is more complicated and the change of shear stiffness with b is not monotonic.

5.2 Parameter $p'_{y,i}$

To illustrate the influence of the size of the initial yield surface defined by $p'_{y,i}$, the soil parameters listed in Table 1, together with $b = 1$ and $\omega = 1$, were adopted. Six different values of $p'_{y,i}$ were assumed and they are 100, 150, 200, 334, 500 and 1,000 kPa. The influence of parameter $p'_{y,i}$ on the simulations is shown in Fig. 7. The effective stress paths simulated follow those in a conventional drained triaxial test in which the axial loading only is increased. The initial stress state for all six cases is the same, with p'=100 kPa and $q = 0$, and the initial voids ratio was $e_i = 1.439$. For this initial soil state and the given intrinsic soil properties, the initial yield surface for the corresponding reconstituted soil is $p'_o = 100$ kPa. Therefore, for the particular situation with $p'_{y,i} = 100$ kPa the soil is in a reconstituted state and has no structure. The soil is structured for situations with $p'_{y,i} > 100$ kPa. Thus, this set of computations simulates the development of structure for soil at constant voids ratio and the same stress state. The following features are simulated.

As indicated in the previous paragraphs, the final state for a structured soil under monotonic shearing with $b > 0$ is the critical state of deformation. Because the final deviatoric stress for all six cases is the same (Fig. 7a), their final states are the same, *i.e.*, the same critical state of deformation with the same stress state and voids ratio. Hence, the final state of a structured soil under monotonic shearing is independent of the size of the initial yield surface.

For soil of a given mineralogy in a given initial condition, *i.e.*, stress state and voids ratio, and tested under a given stress path, a peak strength may or may not be mobilised, depending on the size of the initial yield surface. Consequently, a structured soil may be able to resist a much higher shear stress than the

corresponding reconstituted soil at the same initial stress state and the same voids ratio.

During the softening process the higher the peak strength, the quicker the reduction in the soil strength with the respect to the deviatoric strain. Hence, if softening occurs the peak strength of a structured soil reduces to the critical state strength more rapidly than the corresponding reconstituted soil.

The response pattern usually labelled "dry behaviour" (Schofield and Wroth, 1968) may not be observed for a structured soil, *i.e.*, volumetric expansion may not occur when the softening process starts. It is seen that for the case with $p'_{y,i} = 500$ kPa there is a continuous volumetric compression accompanying the softening process. For the simulation with $p'_{y,i} = 1000$ kPa, volumetric expansion, although observed, starts only after a considerable amount of softening has occurred.

An interesting phenomenon is observed in the simulation with $p'_{y,i} = 334$ kPa. The soil behaves entirely elastically before the stress state reaches the yield surface. When the stress state reaches the point on the yield surface with the critical state stress ratio, virgin yielding also starts (see the inset in Fig. 7a). Because of the special feature of this stress state, the structured soil has no further resistance to shear deformation. However, the volumetric strain increases continuously with the deviatoric strain after this stress state is reached indicating that the soil has not yet reached the critical state of deformation. It reaches a critical state of deformation after the additional voids ratio due to the initial structure is completely diminished.

5.3 Parameter ω

To illustrate the influence of parameter ω, the soil parameters listed in Table 1 were adopted, together with $b = 1$ and $p'_{y,i} = 100$ kPa. The initial stress state is defined as $p' = 100$ kPa and $q = 0$, and the initial value of the additional voids

ratio is $\Delta e_i = 0.8$. Five different values of ω were assumed, i.e., $\omega = 0$, 0.313, 0.625, 0.938 and 1.25 (the corresponding values of $\omega \Delta e_i$ are 0, 0.25, 0.5, 0.75 and 1 respectively). The influence of parameter ω on the simulated behaviour is shown in Fig. 8. The effective stress paths simulated follow those in a conventional drained triaxial test in which the axial loading only is increased. As can be seen from the volumetric deformation, equation (23), parameter ω has no influence on the volumetric strain. In the figure showing the deviatoric and volumetric strain relationship, the variation in this relationship is attributed entirely to the influence of ω on the deviatoric strain. The higher is the value of ω the stiffer is the shear deformation.

Based on the study of the three parameters describing soil structure, it can be concluded that the final state of a structured soil under monotonic shearing, predicted by the proposed model for situations with $b > 0$, is the critical state of deformation. At such a state, the structure of the soil is completely removed. Thus the final state of a structured soil is independent of soil structure and consequently is not influenced by the three new parameters, which describe only the influence of soil structure on soil deformation. The existence of the critical state of deformation for geo-materials and the implication that the associated mechanical properties are independent of material structure have been widely observed features of soil behaviour (*e.g.*, Been and Jefferies, 1985; Ishihara, 1993; Novello *et al*, 1995; Carter *et al*, 2000).

6. Model Evaluation

6.1 Background

The proposed model was also used to simulate the behaviour of soils with structure, and the model was evaluated based on comparisons between the model performance and the corresponding experimental data. The compression behaviour of three different clays is considered first, and they are natural Leda clay, weathered Bangkok clay, and an artificially cemented clay. The shearing

behaviour of three other structured soils was also considered, and they are a natural calcarenite, natural Corinth marl and a natural clay shale.

Two different types of computation were made using the proposed model: simulations and predictions. If the model is used to describe the behaviour of a soil in a particular test or a set of tests and the same experimental data have been employed previously in the determination of the model parameters, this type of computation is defined here as a "simulation". If the model is used to describe the behaviour of a soil in a particular test or a set of tests and all the model parameters have been determined independently of that test or that set of tests, this type of computation is defined as a "prediction".

The following methods were used in the determination of model parameters: (a) values were measured directly from a test and have a physical meaning, (b) use was of empirical equations, (c) some parameters were determined by curve fitting, and (d) others were based on assumed values. For the last method, selection of the value of a parameter is usually based on experience in geotechnical engineering practice. It is proposed that if no experimental data are available the value of parameter ω is determined by the following equation,

$$1-\omega\Delta e_i = 0.5 \ . \tag{34}$$

It may be seen that this assumption implies a mid-range value, based on the constraint conditions imposed on parameter ω, *i.e.*, equation (19).

In all computations the stress units adopted are kPa. In presenting the results of the computations, experimental data for structured soils are represented in the figures by solid circles or squares, which in some cases are linked by thin lines. Data for reconstituted soils are represented by open circles, which in some cases are linked by thin lines. The model simulations are represented by solid lines and those for reconstituted soils by broken lines.

6.2 Compression behaviour of three clays

Three sets of compression tests on different soils are simulated and for these tests only the volumetric deformation has been computed. As can be seen from equation (23), the volumetric deformation is not influenced by the values of parameters ν^* and ω. Hence, there is no need to determine or specify values for these parameters.

6.2.1 Leda Clay

The first group of test data includes five compression tests on natural soft Leda clay performed by Yong and Nagaraji (1977) and Walker and Raymond (1969). The two oedometer tests on the natural and reconstituted Leda clay reported by Yong and Nagaraji (1977) were used to identified soil parameters, and their values are listed in Table 2. The values of parameters λ^* and κ^* and b and $\sigma'_{vy,i}$ were obtained directly from the experimental data. The critical state strength of Leda clay was reported by Walker and Raymond (1969) as $M^* = 1.2$. The intrinsic soil property e^*_{IC} was estimated according to equation (33). It was found from the experimental data (Fig. 9) that e^*_η for one-dimensional compression is equal to 2.353, which gives $e^*_{IC} = 2.338$.

The initial state of the structured soil is $\sigma'_v = 20$ kPa and $e = 1.96$. As shown in Fig. 9, the compression behaviour of Leda clay is well simulated by the model.

Table 2 Model parameters for Leda clay

Parameter	M^*	λ^*	κ^*	e^*_{IC}	b	$\sigma'_{vy,i}$ (kPa)
Value	1.2	0.223	0.03	2.338	1	168.6

Three tests performed by Walker and Raymond (1969) were used to evaluate the model's predictions. Although all the specimens tested by both Yong and Nagaraji (1977) and Walker and Raymond (1969) were Leda clay, they were obtained from different locations in the same area. It is assumed that these specimens differed only in the size of the initial yield surface, *i.e.*, the different

Leda clay samples possessed the same mineralogy and type of structure but may have had different magnitudes of structure. The three compression tests were with $\eta = 0$, 0.63 and 1 respectively. The experimental data for the test with $\eta = 0$ were used to identify the size of the yield surface, and it was found that $p'_{y,i} = 265$ kPa. The predicted compression behaviour of the Leda clay is shown in Fig. 10. For comparison, the virgin isotropic compression line for the reconstituted Leda clay is also represented in the figure by a broken line. It may be observed that the initial voids ratios of the samples for the tests with $\eta = 0.63$ and 1 are essentially the same at the same mean effective stress in the elastic region, but different from that for the test with $\eta = 0$. This indicates that some difference in $p'_{y,i}$ may exist between the first two samples and the third sample. It is seen that the proposed model gives an approximate but reasonable description of the compression behaviour of natural Leda clay.

6.2.2 Bangkok Clay

The second group of test data includes the results of five compression tests on weathered Bangkok clay performed by Balasubramanian and Hwang (1980). The stress ratios for the five tests are 0, 0.16, 0.43, 0.6 and 0.75. The authors were unable to obtain information on the behaviour of reconstituted Bangkok clay. However, the liquid limit value for the clay was 123%, and so the one-dimensional compression curve for the reconstituted soil type was estimated by the empirical method suggested by Burland (1990). Based on the estimated one-dimensional compression curve, values of parameters λ^* and e^*_η for one-dimensional compression were obtained. The isotropic test on the weathered clay was used to identify soil parameters b and $p'_{y,i}$. The critical state strength for the clay was reported by Balasubramanian and Hwang (1980) as $M^* = 0.9$. The intrinsic soil property e^*_{IC} was estimated based on equation (33). The values of these soil parameters are listed in Table 3. The simulated behaviour of Bangkok clay is shown in Fig. 11. It may be noticed that the compression behaviour of the Bangkok clay is well simulated in this case.

Table 3 Model parameters for weathered Bangkok clay

Parameter	M*	λ*	κ*	e^*_{IC}	b	$\sigma'_{vy,i}$ (kPa)
Value	0.9	0.4	0.1	3.82	0.55	35

The predicted compression behaviour of Bangkok clay with $\eta = 0.16$, 0.43, 0.6 and 0.75 is shown in Fig. 12. As may be seen in the inset in Fig. 11, some differences in the initial soil structure exist among the samples used for the five tests. The test specimens were obtained from the field and some variation in the specimens would normally be expected. It may be seen that the initial soil states for the five specimens may be divided into three groups, *i.e.*, the test with $\eta = 0$, the test with $\eta = 0.16$, and tests with $\eta = 0.43$ and 0.6 and 0.75. It is assumed in the simulations that the differences in the initial states of the soil can be represented adequately by the differences in the sizes of the initial structural yield surfaces. It may be seen from the compression curve that the initial stress state for the test with $\eta = 0.16$ is on the yield surface, *i.e.*, $p'_{y,i} = 67.6$ kPa. The size of the initial yield surface for the other three specimens is 45 kPa (the test with $\eta = 0.43$ is used to identify the value of this parameter). Overall, it is seen that the proposed model gives a reasonably good approximation of the compression behaviour of weathered Bangkok clay.

6.2.3 Artificially Cemented Clay

The third group of test data includes the results of five compression tests on an artificially cemented clay performed by Burghignoli *et al* (1998). The soil was composed of a natural Avezzano clay, commercial bentonite, ordinary 425 Portland cement, and distilled water. Homogeneous and fully saturated artificially cemented specimens were made (for details of the sample preparation see the report by Burghignoli *et al*, 1998). Based on two oedometer tests on the reconstituted clay and the structured clay, model parameters were identified and they are listed in Table 4. The authors were not able to obtain data for the critical state strength and a value of M* = 1.2 was assumed, which corresponds to a critical state friction angle of 30°. e^*_{IC} was estimated based on

the proposed equation (33). The behaviour of the clay with structure and in a reconstituted state under cyclic oedometer tests was simulated and the results are shown in Fig. 13. The cyclic compression behaviour of the artificially cemented clay in the oedometer test is well simulated.

Table 4 Model parameters for an artificially cemented clay

Parameter	M*	λ*	κ*	e^*_{IC}	b	$\sigma'_{vy,i}$ (kPa)
Value	1.20	0.505	0.02	5.383	0.7	430

Burghignoli *et al* also performed three sets of compression tests in order to investigate the anisotropic properties of the structured clay generated by anisotropic compression. In one set of these tests, isotropic samples were created. Three of these tests were chosen for prediction. Because at this stage of development the proposed model only takes account of the isotropic properties of a soil with and without structure, it would not be meaningful to examine the performance of the model in describing the anisotropic behaviour of soil.

The three identical samples were loaded isotropically from stress state A (Fig. 14) with $p' = 25$ kPa and $e_i = 3.5$ to state B with $p' = 300$ kPa. They were unloaded isotropically to state C with $p' = 140$ kPa. Subsequently, the first sample was loaded again isotropically. The second sample was sheared with constant mean effective stress to a state D with $p' = 140$ kPa and $q = 75$ kPa. This sample was then loaded at constant η, *i.e.*, $\eta = 0.5$. The third sample was sheared with constant mean effective stress to a state E with $p' = 140$ kPa and $q = 140$ kPa. This sample was then loaded at constant η, *i.e.*, $\eta = 1$. The stress paths for the three tests are shown schematically in the inset to Fig. 14.

The size of the initial yield surface, identified from the isotropic test, is $p'_{y,i} = 212$ kPa. The value of $p'_{y,i}$ for this set of tests is much smaller than that obtained from the oedometer test, but it should be noted that the samples in

these two sets of tests were different. It was observed that the yield surface for the structured clay after the initial virgin loading to the isotropic stress state B with $p' = 300$ kPa, plus subsequent isotropic unloading and reloading along stress path BCB, is 340 kPa, a value larger than the maximum yield stress the soil has ever experienced. This phenomenon has been confirmed by Burghignoli *et al* (1998) as a material property for this artificially structured clay and it is highly likely that it is associated with the development of soil structure during the duration of the test, perhaps due to the ageing effect of the cement. In the prediction, this development of soil structure was considered by choosing $p'_{y,i} = 340$ kPa for the clay for reloading after point C.

The simulation of the isotropic test and the predictions for the two tests with constant shear stress ratio are shown in Fig. 14. It is seen that the proposed model gives an approximate but reasonable description of the compression behaviour of the artificially structured clay.

In this section, descriptions of how the model was employed to simulate and predict the compression behaviour of structured soils have been presented. Overall, it may be concluded that the proposed model provides a good qualitative description of the soil behaviour, but the quantitative description is only approximate. In the selection of experimental data for model evaluation, only tests performed on structured soil with isotropic mechanical properties were selected because the current version of the model does not allow for anisotropic behaviour of the soil.

6.3 Behaviour of a natural calcarenite

Results of the experimental work carried out by Lagioia and Nova (1995) on a natural calcarenite have been compared with the model predictions and simulations. The natural calcarenite was formed by marine deposition. It is a coarse-grained material with a high degree of uniformity and calcareous inter-particle cement. An isotropic compression test on the soil was used to identify

soil parameters and their values are listed in Table 5. The isotropic compression behaviour of the calcarenite and its simulation are shown in Fig. 15.

Table 5 Model parameters for a natural calcarenite

Parameter	M*	λ*	κ*	e^*_{IC}	ν*	b	ω	$p'_{y,i}$ (kPa)
Value	1.45	0.208	0.0165	2.57	0.25	30	3.33	2400

The values of parameters e^*_{IC} and λ* and κ* and b and $p'_{y,i}$ were obtained directly from the experimental data. The value of Poisson's ratio was assumed. The critical state strength for the natural clacarenite was reported by Lagioia and Nova (1995) as M* = 1.45. The initial state for the structured soil is defined by p' = 147 kPa and e = 1.148. Thus, the initial value of the additional voids ratio sustained by the soil structure is found as $\Delta e_i = 0.15$. The value of parameter ω was estimated using equation (34).

By using the values of the model parameters listed in Table 5, the behaviour of the natural calcarenite under conventional drained triaxial tests was predicted. There are eight tests in total and the stress paths for the predictions are as follows. Firstly, the soil was loaded or unloaded isotropically from the initial isotropic state with p' = 147 kPa and e = 1.148 to the chosen state, *i.e.*, p' = 25, 200, 400, 600, 900, 1,100, 2,000 and 3,500 kPa. The confining pressure σ'_3 was then kept constant and the axial loading was increased until failure of the sample was observed. The test results and the predictions are shown in Figs 16 to 24. For the test with σ'_3 = 3,500 kPa, the initial stress state is much larger than the size of the initial structural yield surface. According to the proposed model, the structure of the soil at σ'_3 = 3,500 kPa is actually completely destroyed since the soil has a very high destructuring index, *i.e.*, b = 30. Thus, the soil in this test behaves as a reconstituted material throughout this test. Destructuring of this sample was confirmed by Lagioia and Nova (1995). Considering the wide range of initial stresses, it is seen that the proposed model

gives a successful prediction of the behaviour of this natural and highly structured calcarenite.

Simulations of the behaviour of the calcarenite have also been made, where a part of the test data was employed to determine the model parameters. The values of the model parameters used for the simulations (as opposed to "predictions") are listed in Table 6. Comparison with values listed in Table 5 reveals that the values for the following parameters are different: e^*_{IC}, κ^* (or K^*), ν^*, ω and $p'_{y,i}$. In the previous predictions the values for parameters ν^* and ω were assumed. In these simulations, the value for ν^* suggested by Lagioia and Nova (1995) was adopted, while the value for ω was obtaining by curve fitting. In Table 6, a value of Young's modulus E^* is given, instead of a value for κ^*. It was observed by Lagioia and Nova (1995) that the pre-yielding behaviour of the calcarenite, although elastic, is not linear in the e-lnp' coordinates. Hence, a constant parameter κ^* over the full range of stress explored is inappropriate for this material, and so Lagioia and Nova suggested a constant Young's modulus, *i.e.*, E^* = 76,923 kPa. Based on the definition of the Young's modulus and that for parameter κ^*, the following relationship between E^* and κ^* is obtained

$$\kappa^* = \frac{3(1+e)(1-2\nu^*)p'}{E^*} \quad . \tag{35}$$

Because the mean effective stress p' generally varies during a test and E^* is now considered as a material constant, κ^* is actually a variable, rather than a constant. However, the basic equations of the proposed model, such as those given by equations (15), (23) and (24), were derived based on the assumption that both the virgin yielding behaviour and the elastic behaviour of a soil under isotropic loading are linear in the e - lnp' coordinates. Therefore, in order to employ the equations of the Structured Cam Clay model for these simulations, different values of the "constant" parameter κ^* were determined for each

individual test, according to equation (35). It is necessary to make such an approximation in order to retain use of this relatively simple constitutive model.

It is obvious that the constitutive equations of the proposed model can be reformulated so that the linear elastic behaviour of soil in the e – p' space can be modelled accurately. A method for such formulation can be found from a paper by Liu and Carter (2001). The reformulation is not introduced in this paper. The above approximate method is suggested instead. The idea for this approximation is widely used in geotechnical engineering, and is consistent with the method of stress path analysis (Lambe, 1964; Wood, 1984).

In order to determine the "constant" value of κ^* for a particular test, a particular value of p' must be selected for substitution into equation (35). The value of the initial mean effective stress is an obvious and also the simplest choice. However, an average value of the mean effective stress may be more appropriate, but this selection would cause difficulty in many applications because the stress paths of soil elements are usually not known *a priori*. In the simulations considered here, the stress paths of the tests are known. Hence, the average value of p' for the stress path from the initial stress state to the state at the yield surface was used to compute κ^* for each individual test.

A revised value of parameter e^*_{IC} was determined based on a comparison between the predictions and the experimental data in the e-lnp' coordinates (Fig. 25). It is seen that the measured final state of the soil during monotonic shearing does not fall onto the critical state line predicted by the model, but rather falls onto a line below and parallel to the predicted critical state line. The difference between the two lines in the vertical direction can be measured from the figure and it is found that $\Delta e = 0.187$. Therefore, the value for e^*_{IC} was modified as $e^*_{IC} = 2.57 - 0.187 = 2.383$ for the simulations.

The initial yield surface for the calcarenite adopted in the predictions is an ellipse with the aspect ratio being M* and the size defined by $p'_{y,i} = 2{,}400$ kPa,

as identified from the isotropic compression test. The actual initial yield points for the soil measured by Lagioia and Nova (1995) are shown in Fig. 26. It is found that the initial yield points constitute approximately an ellipse, with an aspect ratio being 1.12, different from that of the critical state strength. In the simulations the latter value of the aspect ratio was adopted only for determination of the initial yield points.

Table 6 Revised values of model parameters for a natural calcarenite

Parameter	M*	λ*	**E*** ***(kPa)***	e^*_{IC}	ν*	B	ω	$p'_{y,i}$ (kPa)
Value	1.45	0.208	76,923	2.383	0.13	30	3	2,400 kPa; the aspect ratio of the yield surface = 1.12.

Comparisons between the theoretical simulations and the experimental data are also shown in Figs 16 to 24. The simulations are represented by broken lines. The range of the variation of the mean effective stress simulated for this series of tests is from 25 kPa to 3,500 kPa and the structure of the soil varies from intact to completely destructured. It can be seen that the behaviour of the natural calcarenite has been simulated satisfactorily with one set of revised model parameters (given that κ* varies from test to test while E^* is held constant).

A qualitative difference is observed between the experimental data and the predictions during the softening and destructuring of the calcarenite (*e.g.*, see Figs 16, 17 and 18). It is observed in the experiments that after softening starts the strength of the calcarenite immediately drops to a very low value, near the final critical state strength. After this reduction of the soil strength the deviatoric stress and strain relationship is basically flat. According to Lagioia and Nova's explanation (Lagioia and Nova, 1995), the immediate drop of soil strength is attributed to the fact that the structure of the calcarenite is not stable. Lagioia and Nova (1995) explained that even during an isotropic compression test the structure of this soil is removed immediately and completely when the

soil is loaded to a virgin yield stress state. They observed that during destructuring the mean effective stress was actually reduced by a small amount in the strain-controlled test. That is to say, this particular structure of the calcarenite cannot sustain the initial yield stress without destructuring when the soil is loaded to that stress state. However, for the shearing tests shown in Figs. 16 and 17 and 18, the data indicate that the capacity of the structured soil to sustain additional voids ratio is not diminished in step with the shear strength of the soil. It may also be observed that there is no great amount of volumetric deformation during the whole softening process. Why the capacity to sustain additional voids ratio associated with soil structure does not diminish in step with the reduction in soil strength appears to need further investigation.

In the predictions, destructuring occurs as the material softens. Because of the highly sensitive nature of the soil structure, the deformation of the soil at the beginning of the softening is dominated by destructuring and the destructuring is completed within a small decrease of stress, or shrinkage of the yield surface. Consequently, it is predicted that there is basically a flat deviatoric stress and strain curve after the occurrence of softening. After the structure of the soil is removed, some softening continues and the reduction of soil strength from the peak strength to the critical state strength is achieved mainly during this period of deformation. The model predicts consistently that the additional voids ratio sustained by soil structure is reduced to zero in accordance with the destructuring.

A conclusion may be drawn about the qualitative difference between the experimental data and the predictions of destructuring during softening. The proposed model is suitable to describe the destructuring of soil resulting from a variation of stress, but not the instability of soil structure, *i.e.*, catastrophic collapse of structure the moment the soil reaches a virgin yield stress state. The authors have studied the destructuring of over fifty different naturally and artificially structured soils from over a dozen of countries, and found almost all

the soil structures are relatively stable and are capable of sustaining the initial yield stress under isotropic and one-dimensional compression (Liu and Carter 1999, 2000; Liu *et al.* 2000). From these observations it is deduced that the mechanism of destructuring proposed in the model is valid for most soils found in situ.

6.4 Behaviour of Corinth marl

Results of the experimental work performed by Anagnostopoulos *et al* (1991) on a natural Corinth marl have been compared with the model simulations. Two sets of tests were reported: a set of three isotropic compression tests on both natural and reconstituted Corinth marl, and a set of five shearing tests on the intact and partially destructured soil. From the first set of tests, the soil parameters e^*_{IC}, λ^*, κ^*, b and $p'_{y,i}$ have been identified, and their values are listed in Table 7. The measured and simulated behaviour of the soil in isotropic compression is shown in Fig. 27. Two isotropic compression tests on reconstituted Corinth marl are reported, and some small discrepancies on the isotropic compression line are observed between the two test samples, which were assumed to be identical. For most natural soils, *i.e.*, not artificially manufactured samples, some discrepancy in the stress and strain behaviour is expected due to material variance. The isotropic test which gave the better simulation of the shearing behaviour of the Corinth marl was selected for identifying the model parameters.

The initial value of the additional voids ratio, *i.e.*, Δe_i, was found to be 0.102. The value of parameter ω was estimated based on equation (34). The value of Poisson's ratio was assumed as 0.25. The critical state strength M* was determined based on the second set of tests, *i.e.*, the final strength of the soil reached under monotonic shearing. The value of M* is the only parameter determined from the data from the shearing tests. The behaviour of the intact and partially destructured soil during conventional drained triaxial compression

tests was simulated, based on the values of model parameters listed in Table 7. Both the simulations and the experimental data are shown in Fig. 28.

Table 7 Model parameters for natural Corinth marl

Parameter	M*	λ*	**κ***	e^*_{IC}	ν*	b	ω	$p'_{y,i}$ (kPa)
Value	1.38	0.04	0.008	0.775	0.25	0.4	4.9	3,800 kPa

For all five compression tests, the confining pressures were kept constant at 98, 294, 903, 1,500 and 4,000 kPa respectively, and the axial loading was increased until the specimens failed. The initial state of the soil was obtained from the isotropic test reported by Anagnostopoulos *et al* (1991), as shown in Fig. 27, with $p' = 34.6$ kPa and $e = 0.585$. The initial states of the specimens for the four tests were calculated based on the proposed model. They are: $p' = 98$ kPa and $e = 0.577$, $p' = 294$ kPa and $e = 0.568$, $p' = 903$ kPa and $e = 0.559$, $p' = 1{,}500$ kPa and $e = 0.555$ and $p' = 4{,}000$ kPa and $e = 0.543$. For the first four tests, the initial stress state of the soil was within the initial structural yield surface, defined by $p'_{y,i} = 3{,}800$ kPa, and therefore the soil samples for these tests are assumed to be intact. For the fifth test, the initial stress state of the soil exceeds the initial structural yield surface and the soil sample has experienced partial destructuring. It is seen that the proposed model gives a reasonable representation of the behaviour of the highly structured, stiff Corinth marl.

6.5 Behaviour of La Biche clayshale

Results of the experimental work performed by Wong (1980) on a natural clayshale have been compared with the model simulations. The clayshale specimens were obtained by core sampling. The soil is a highly over-consolidated, compacted shale. The water content for the natural shale was between 11.5% and 12.4% with an average water content of 12.1%. Three conventional drained triaxial tests on the natural clayshale were simulated in order to demonstrate the capability of the proposed model. The values of model

parameters employed for the simulation are listed in Table 8. A comparison between the simulations and the experimental data is shown in Fig. 29. For all the tests, the confining pressures were kept constant at 50, 250 and 500 kPa respectively.

Table 8 Model parameters for a natural clayshale

Parameter	M*	λ*	**E* *(kPa)***	e^*_{IC}	ν*	b	ω	$p'_{y,i}$ (kPa)
Value	1.45	0.06	73,000	0.668	0.25	0.2	4	3,800 kPa

The values of parameters M* and $p'_{y,i}$ and E^* were obtained from the experimental data. It can be observed from Fig. 29(a), that the shear behaviour of the clayshale before the peak strength is reached is essentially independent of the initial confining pressure. Consequently, the behaviour of the soil before the peak strength can be interpreted as elastic and the elastic shear modulus is constant. The value of Poisson's ratio was assumed to be 0.25. Based on the elastic shear modulus of the clayshale and the value of ν*, the Young modulus for the soil was found as E^* = 73,000 kPa. The values of λ*, e^*_{IC}, b and ω were determined by best fitting.

The initial water content for the clayshale at p' = 50 kPa was assumed to be 12.1%, the average water content of the soil at natural state, and so the initial sate is given by p' = 50 kPa and e = 0.327. Thus the initial voids ratio sustained by the soil structure can be calculated as Δe_i = 0.076. The initial states for the soil in the other two tests were calculated to be p' = 250 kPa, e = 0.322, and p' = 500 kPa, e = 0.317.

As explained previously, adopting a constant value of E^* overall implies a value of κ* that varies between tests. The following values were used here: κ* = 0.005 for the test with σ'_3 = 50 kPa, κ* = 0.012 for the test with σ'_3 = 250 kPa, and κ* = 0.02 for the test with σ'_3 = 500 kPa.

It is seen from Fig. 29 that the proposed model has the capability of modelling the behaviour of this structured clayshale. For the clayshale in the test with σ'_3 = 500 kPa, the volumetric deformation remains compressive even though the shear strength of the soil softens from a peak of 2,600 kPa to 1,800 kPa. This type of behaviour has been widely observed in structured clays and clayshales (*e.g.*, Bishop *et al*, 1965; Lo, 1972; Georgiannou *et al*, 1993; Robinet *et al*, 1999; Carter *et al*, 2000).

7. Conclusion

The Modified Cam Clay model has been generalised so that the isotropic variation of the mechanical properties resulting from the presence of soil structure can be described. A new hierarchal model, referred to as the Structured Cam Clay model, was proposed. Besides the original five parameters introduced in the Modified Cam Clay model, three new parameters have been introduced. They are: b, the destructuring index, $p'_{y,i}$, the size of the initial structural yield surface, and ω, a parameter describing the effect of soil structure on the plastic flow rule. Values of the first two parameters can be determined from an isotropic compression test or an oedometer test. The third parameter can be determined from the volumetric strain and deviatoric strain curve obtained from a shearing test.

Overall, the proposed model has been used to predict both the compression and shearing behaviour of six structured soils. The computations cover a wide range of stress, initial voids ratio and soil structure, both naturally and artificially formed. It has been demonstrated that the proposed model describes successfully many important features of the behaviour of structured soils and has improved significantly the performance of the Modified Cam Clay model by quantifying the important influence of soil structure. In particular, the fact that the new model is able to predict simultaneous material softening and

compressive volumetric strain is considered to be a distinct advantage of the new model over Modified Cam Clay.

Because the Modified Cam Clay model is the basis of the new model, obviously the new model is suitable only for those soils for which the behaviour of the reconstituted materials can be described adequately by Modified Cam Clay. Anisotropic features of soil behaviour, either due to the reconstituted parent soil or due to the presence of soil structure, were not studied in this paper, but will be the topics of future research.

This paper has concentrated on introducing the new model and its basic features, and therefore only the behaviour of soil under fully drained conditions has been considered. The authors also plan a future investigation of the performance of the model for undrained conditions and a systematic study on the identification of model parameters from tests commonly carried out by engineers in geotechnical practice.

8. Acknowledgements

Some of the work described here forms part of the research program of the Special Research Centre for Offshore Foundation Systems, established and supported under the Australian Research Council's Research Centres Program. In addition, a Large Grant from the Australian Research Council in partial support of this work is also gratefully acknowledged.

9. References

Anagnostopoulos A. G., Kalteziotis N., Tsiambaos G. K., and Kavvadas M. (1991), "Geotechnical properties of the Corinth Canal marls", *Geotechnical and Geological Engineering*, Vol. 9(1), pp.1-26.

Arces M., Nocilla N., Aversa S. and Cicero G. L. (1998), "Geological and geotechnical features of the Calcarenite di Marsala", *The Geotechnics of Hard Soils - Soft Rocks*, Evangelista and Picarelli (eds), pp.15-25.

Balasubramaniam A. S. and Hwang Z. M. (1980), "Yielding of weathered Bankok clay", *Soils and Foundations*, Vol. 20(2), pp.1-15.

Been K. and Jefferies M. G. (1985), "A state parameter for sands", *Géotechnique*, Vol. 35(1), pp.99-112.

Bishop A. W., Webb D. L., and Lewin P. I. (1965), "Undisturbed samples of London clay from the Ashford Common shaft: strength-effective stress relationship", *Géotechnique*, Vol. 15(1), pp.1-13.

Britto A. M. and Gunn M. J. (1987), *Critical State Soil Mechanics via Finite Elements*, Chichester: Ellis Horwood Ltd.

Burland J. B. (1990), "On the compressibility and shear strength of natural soils", *Géotechnique*, Vol. 40(3), pp.329-378.

Burland J. B., Rampello S., Georgiannou V. N., and Calabresi G. (1996), "A laboratory study of the strength of four stiff clays", *Géotechnique*, Vol. 46(3), pp.491-514.

Burghignoli A., Milizaano S., and Soccodato F. M. (1998), "The effect of bond degradation in cemented clayey soils", *The Geotechnics of Hard Soils - Soft Rocks*, Evangelista and Picarelli (eds), pp.465-472.

Carter J. P., Airey D. W. and Fahey M. (2000), "A review of laboratory testing of calcareous soils', *Engineering for Calcareous Sediments*, Al-Shafei (*ed*), Vol. 2, pp.401-431.

Cotecchia F. and Chandler R. J. (1997), "The influence of structure on the pre-failure behaviour of a natural clay", *Géotechnique*, Vol. 47(3), pp.523-544.

Cuccovillo T. and Coop M. R. (1999), "On the mechanics of structured sands", *Géotechnique*, Vol. 49(6), pp.741-760.

Dafalias Y. F. (1987), "An anisotropic critical state clay plasticity model", *Proc*. 2nd Int. Conf. On Constitutive Laws for Engineering Materials, Tucson, Arizona, Vol. 1, pp.513-521.

Gens A. and Potts D. M. (1988), "Critical state models in computational geomechanics", *Engineering Computation*, Vol. 5, pp.178-197.

Gens A. and Nova R. (1993), "Conceptual bases for a constitutive model for bonded soils and weak rocks", *Geotechnical Engineering of Hard Soils – Soft Rocks*, Anagnostopoulos *et al* (*ed*), Vol. 1, pp.485-494.

Georgiannou V. N., Burland J. B., Hight D. W. (1993), "The behaviour of two hard clays in direct shear", *Geotechnical Engineering of Hard Soils – Soft Rocks*, Anagnostopoulos *et al* (*ed*), Vol. 1, pp.501-507.

Graham J. and Li C. C. (1985), "Comparison of natural and remoulded plastic clay", *J. Geotechnical Engineering*, ASCE, Vol. 111(7), pp.865-881.

Ishihara K. (1993), "Liquefaction and flow failure during earthquakes", *Géotechnique*, Vol. 43(3), pp.351-415.

Jacky J. (1944), "The coefficient of earth pressure at rest", *J. of the Society of Hungarian Engineers and Architects*, Budapest, pp.355-358.

Kavvadas M. and Amorosi A. (2000), "A constitutive model for structured soils", *Géotechnique*, Vol. 50(3), pp.263-273.

Lagioia R. and Nova R. (1995), "An experimental and theoretical study of the behaviour of a calcarenite in triaxial compression", *Géotechnique*, Vol. 45(4), pp.633-648.

Lambe T. W. (1964), "Method of estimating settlement", *J. Geotechnical Engineering*, ASCE, Vol. 90, pp.43-67.

Leroueil S. and Vaughan P. R. (1990), "The general and congruent effects of structure in natural soils and weak rocks", *Géotechnique*, Vol. 40(3), pp.467-488.

Liu M. D. and Carter J. P. (1999), "Virgin compression of structured soils", *Géotechnique*, Vol. 49(1), pp.43-57.

Liu M. D. and Carter J. P. (2000), "Modelling the destructuring of soils during virgin compression", *Géotechnique*, Vol. 50(4), pp.479-483.

Liu M. D., Carter J. P., Desai C. S. and Xu K. J. (2000), "Analysis of the compression of structured soils using the disturbed state concept", *Int. J. for Numerical and Analytical Methods in Geomechanics*. Vol. 24, pp.723-735.

Liu M. D. and Carter J. P. (2001), "A conceptual framework for modelling the mechanical behaviour of structured soils", *Computer Methods and Advances in Geomechanics*, edts Desai, Kundu, Harpalani, Contractor & Kemeny, Vol. 1, pp.347-354.

Liu M. D. and Carter J. P. (2002), "A structured Cam Clay Model", Research Report, University of Sydney.

Lo K. Y. (1972), "An approach to the problem of progressive failure", *Canadian Geotechnical. J.*, Vol. 9(4), pp.407-429.

Muir-Wood D. (1990), *Soil Behaviour and Critical State Soil Mechanics*, Cambridge University Press.

Nambiar M. R. M., Rao G. V., and Gulhati S. K. (1985), "The nature and engineering behaviour of fine-grained carbonate soil from off the west coast of India", *Marine Geotechnology*, Vol. 6(2), pp.145-171.Novello E. and Johnston I. W. (1995), "Geotechnical materials and the critical state", *Géotechnique*, Vol. 45(2), pp.223-235.

Novello E. and Johnston I. W. (1995), "Geotechnical materials and the critical state", *Géotechnique*, Vol. 45(2), pp.223-235.

Olson R. E. (1962), "The shear strength properties of calcium illite", *Géotechnique*, Vol. 12(1), pp.23-43.

Potts D. M. and Zdravkovic L. (1999), *Finite Element Analysis in Geotechnical Engineering: Theory*, London, Thomas Telford.

Robinet J. C., Pakzad M., Jullien A., and Plas F. (1999), "A general modelling of expansive and non-expansive clays", *Int. J. Numerical and Analytical Method in Geomechanics*, Vol. 23, pp.1319-1335.

Roscoe K. H. and Burland J. B. (1968), "On the generalised stress-strain behaviour of 'wet clay' ", *Engineering Plasticity*, Heyman and Leckie (*ed*), pp.535-609.

Rouainia M. and Muir Wood D. (2000), "A kinematic hardening model for natural clays with loss of structure", *Géotechnique*, Vol. 50(2), pp.153-164.

Schofield A. N. and Wroth C. P. (1968), *Critical State Soil Mechanics*, MacGraw-Hill, London.

Walker L. K. and Raymond G. P. (1969), "The prediction of consolidation rates in a cemented clay", *Canadian Geotechnical J.*, Vol. 6(4), pp.193-216.

Wheeler S. J. (1997), "A rotational hardening elasto-plastic model for clays", *Proc.* 14th Int. Conference Soil Mechanics and Foundation Engineering, Vol. 1, pp.431-434.

Whittle A. J. (1993), "Evaluation of a constitutive model for overconsolidated clays", *Géotechnique*, Vol. 43(2), pp.289-314.

Whittle A. J. and Kavvadas M. J. (1994), "Formulation of MIT-E3 constitutive model for overconsolidated clays", *Journal of Geotechnical Engineering*, ASCE, Vol. 120(1), pp. 199-224.

Wong R. C. K. (1980), "Swelling and softening behaviour of La Biche shale", *Canadian Geotechnical J.*, Vol. 35, pp.206-221.Yong R. N. and Nagaraj T. S. (1977), "Investigation of fabric and compressibility of a sensitive clay", *Proc.* Int. Symposium on Soft Clay, Asian Institute of Technology, pp.327-333.

Wood D. M. (1984), "Choice of models for geotechnical predictions", *Mechanics of Engineering Materials*, Desai & Gallagher (*ed*), pp.633-654.

Yu H. S. (1998), "CASM: a unified state parameter model for clay and sand", *Int. J. Numerical Analytical Method in Geomechanics*, Vol. 22(8), pp.621-653.

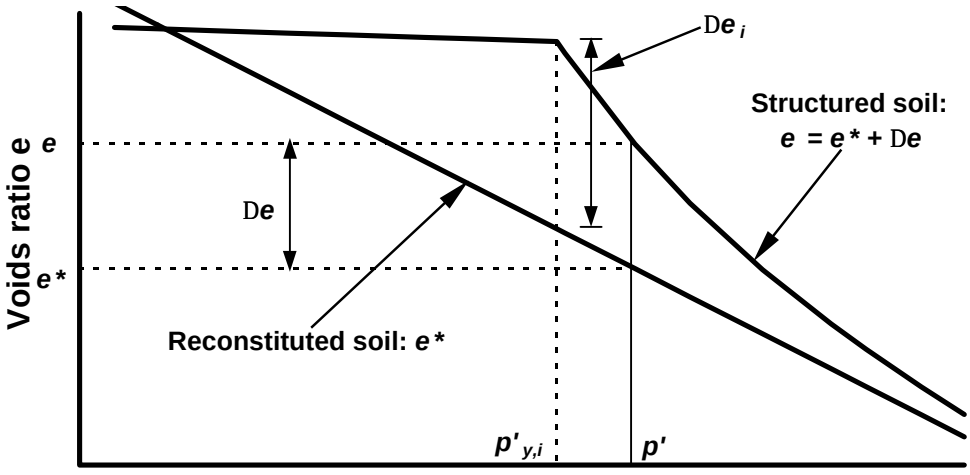

Fig. 1 Idealization of the isotropic compression behaviour of reconstituted and structured soils

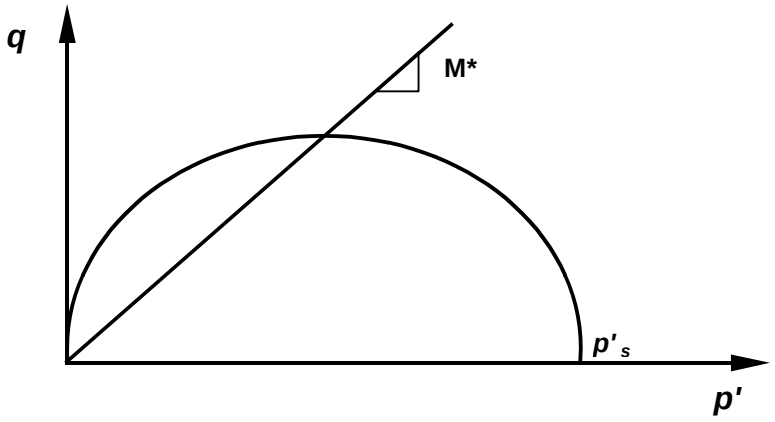

Fig. 2 The yield surface for structured soils

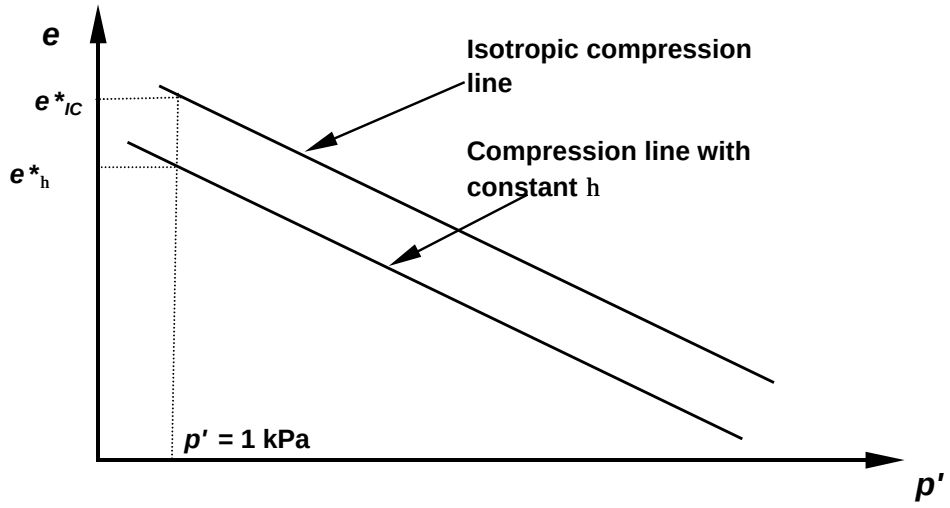

Fig. 3 Compression behaviour of reconstituted clay based on Critical State Soil Mechanics

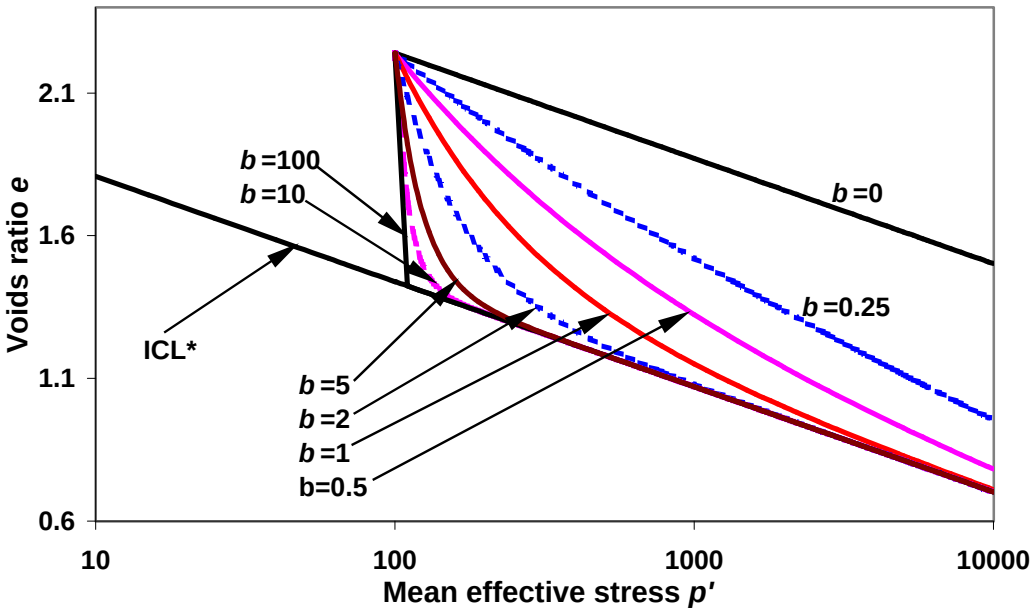

Fig. 4 Influence of parameter *b* on isotropic compression behaviour

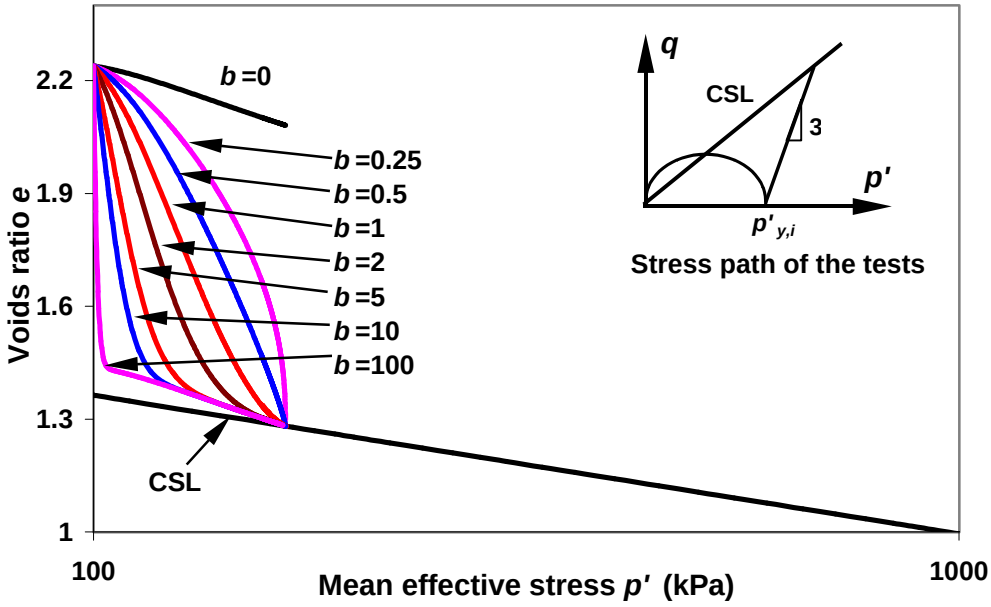

Fig. 5 Influence of destructuring index *b* on the shearing behaviour of soil in the *e*-*p′* space

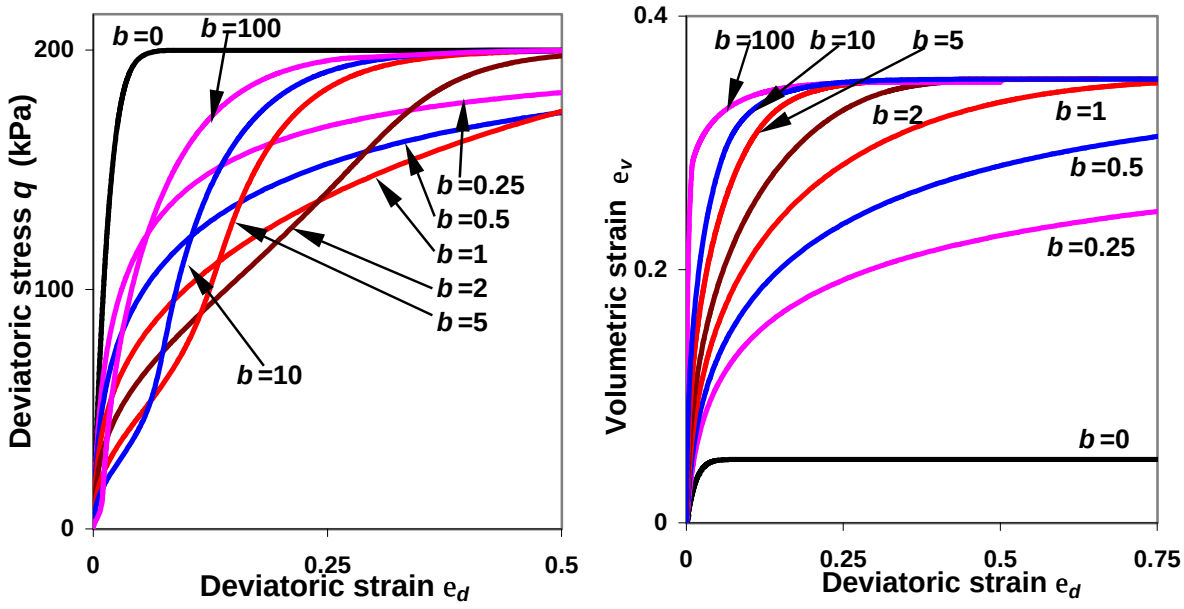

(a) Stress and strain relationship

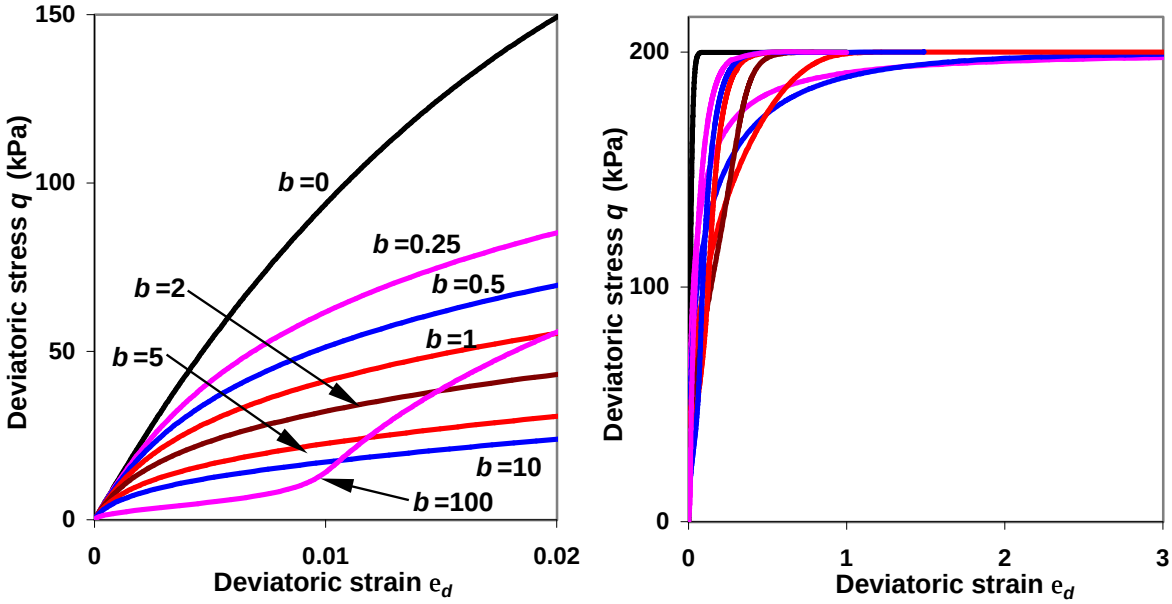

(b) Deviatoric stress and strain relationship at different scales

Fig. 6 Influence of destructuring index *b* on the shearing behaviour of soil

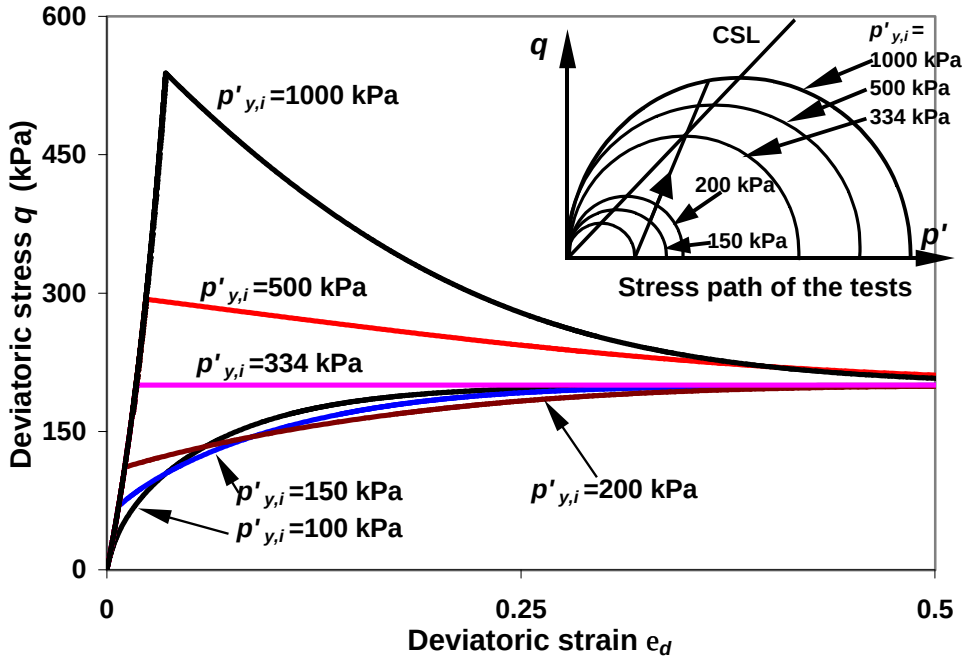

(a) Deviatoric stress and strain

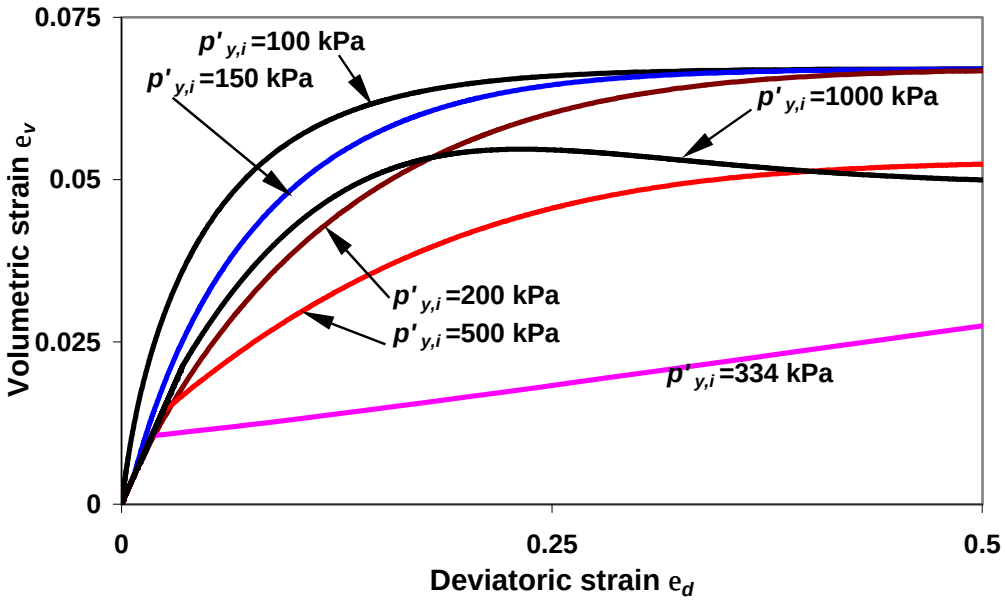

(b) Deviatoric and volumetric strains

Fig. 7 Influence of the size of the initial yield surface on simulated soil behaviour

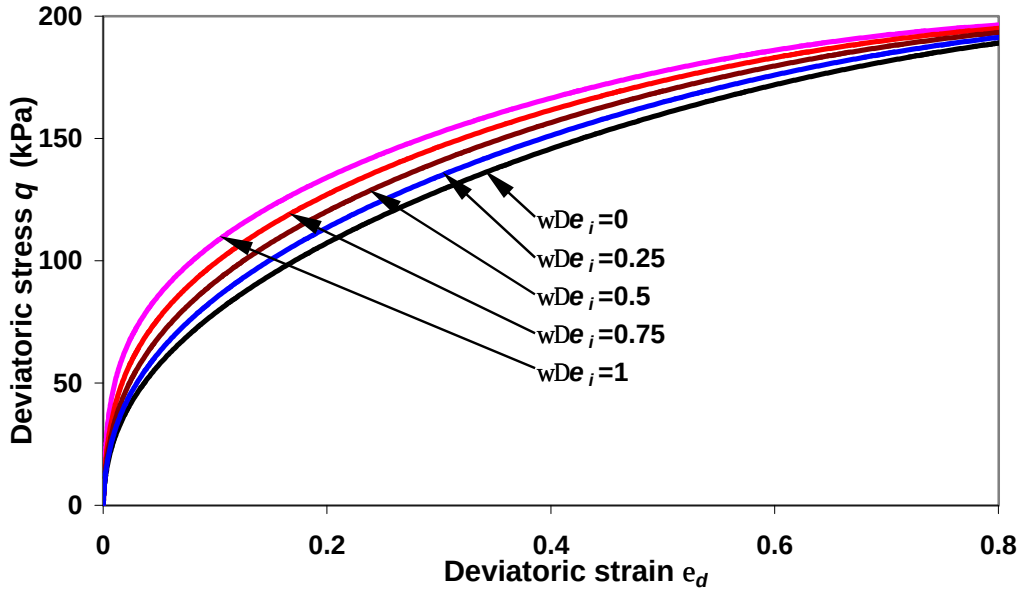

(a) Deviatoric stress and strain

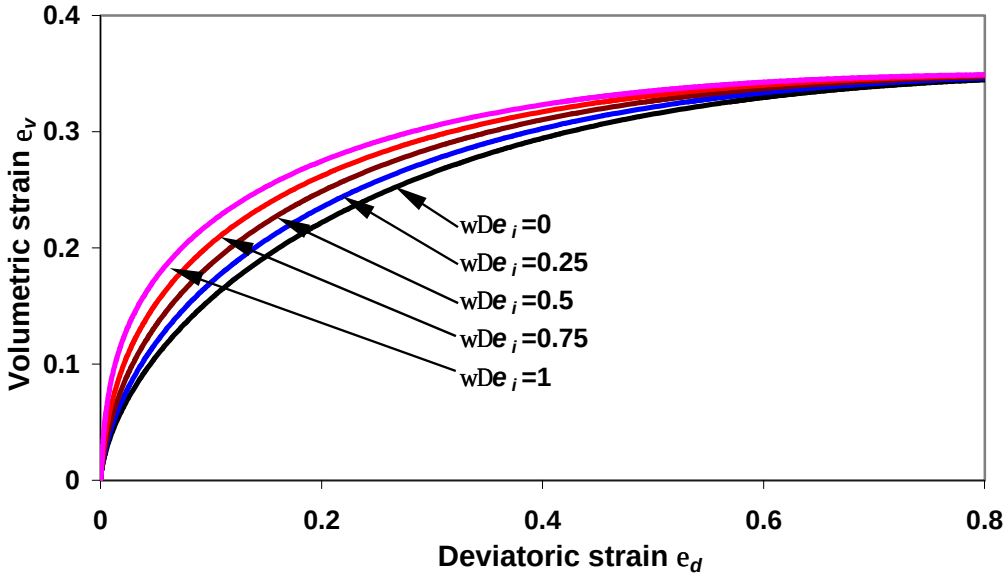

(b) Deviatoric and volumetric strains

Fig. 8 The Influence of parameter w on soil behaviour simulated

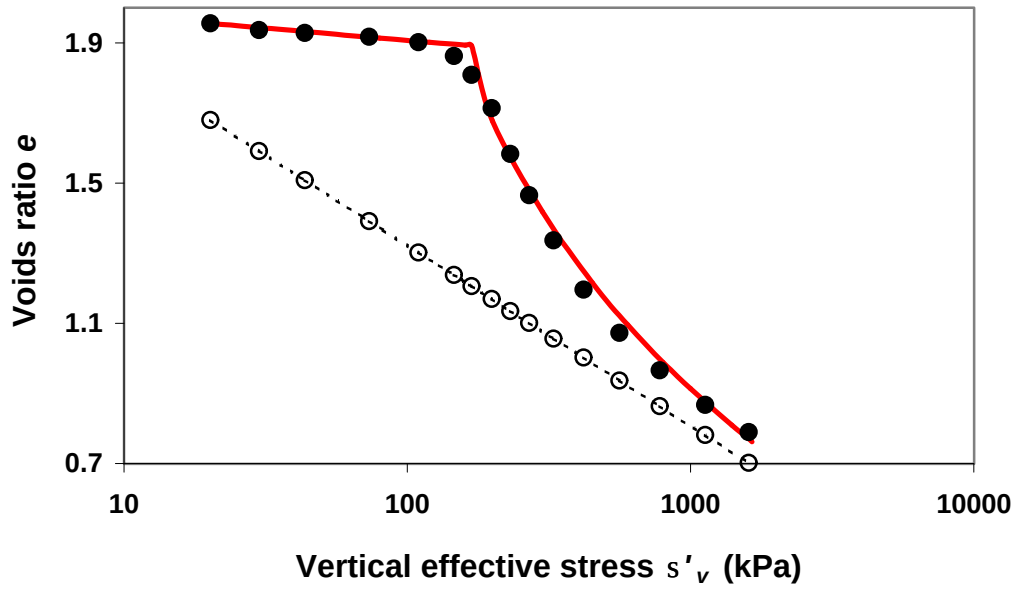

Fig. 9 Behaviour of Leda clay in an oedometer test (Test data after Yong ang Nagaraji, 1977)

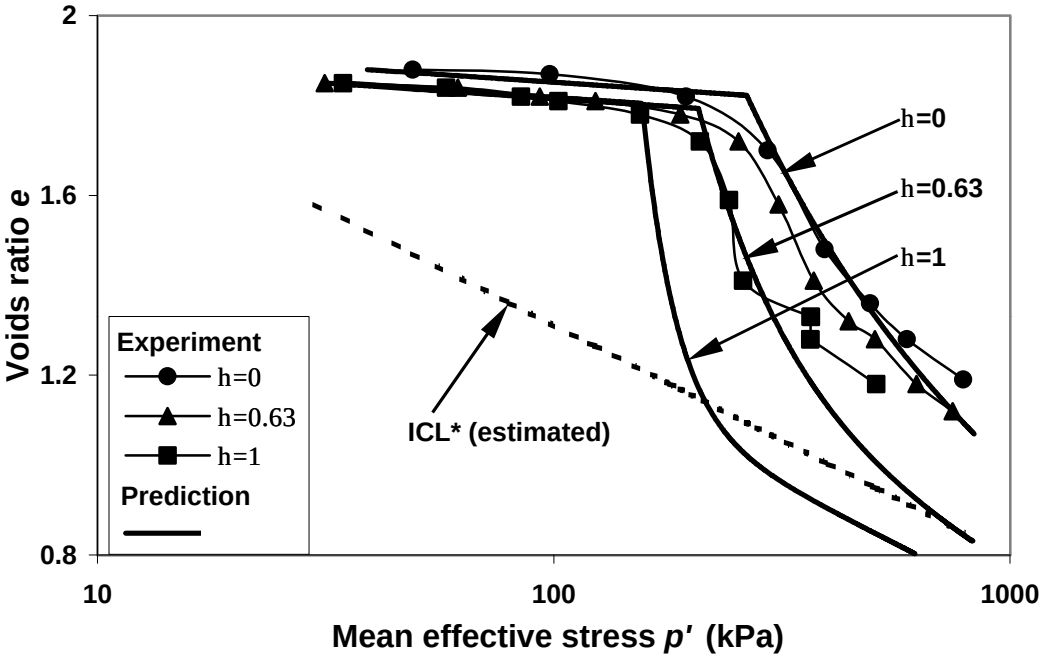

Fig. 10 Compression behaviour of Leda clay with different values of h (Test data after Walker and Raymond, 1969)

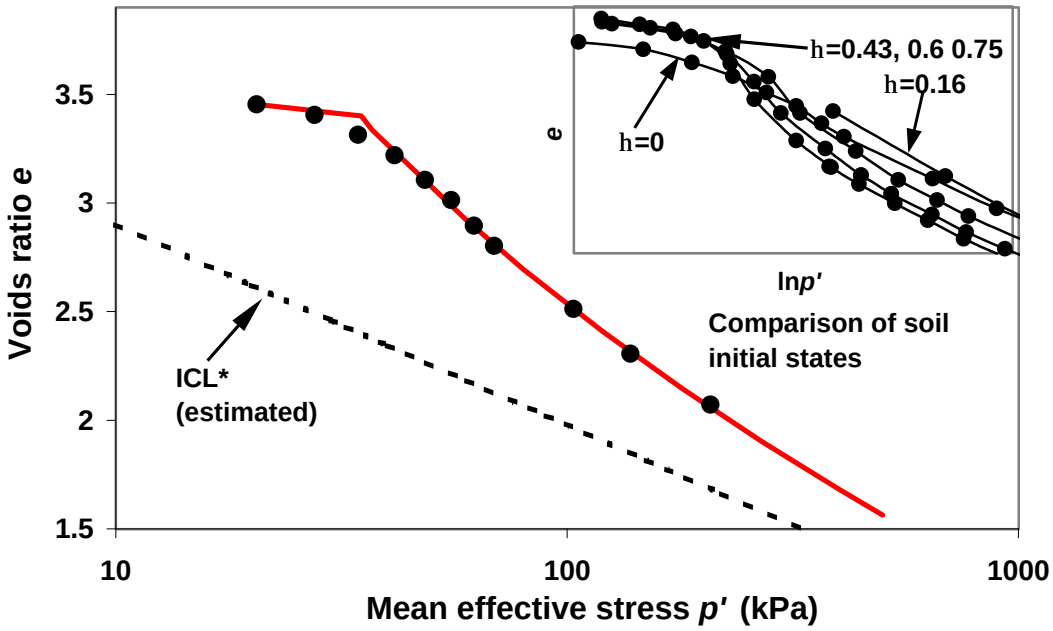

Fig. 11 Isotropic compression behaviour of weathered Bankok clay (Test data after Balasubramanian and Hwang, 1980)

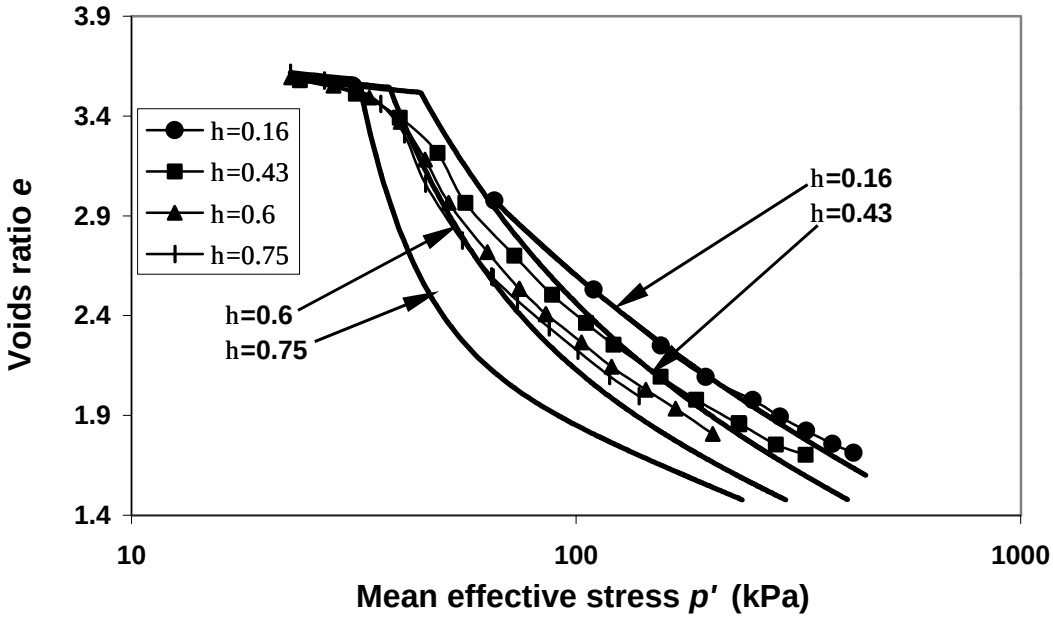

Fig. 12 Compression behaviour of weathered Bankok clay (Test data after Balasubramanian and Hwang, 1980)

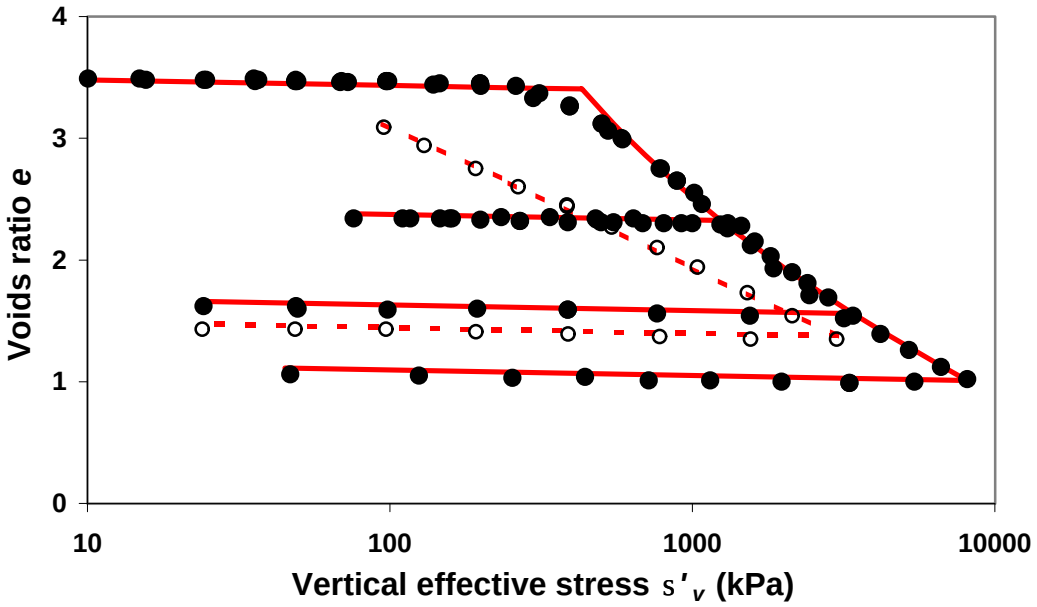

Fig. 13 Oedometer tests on an artificially cemented clay (Test data after Burghignoli *et al* , 1998)

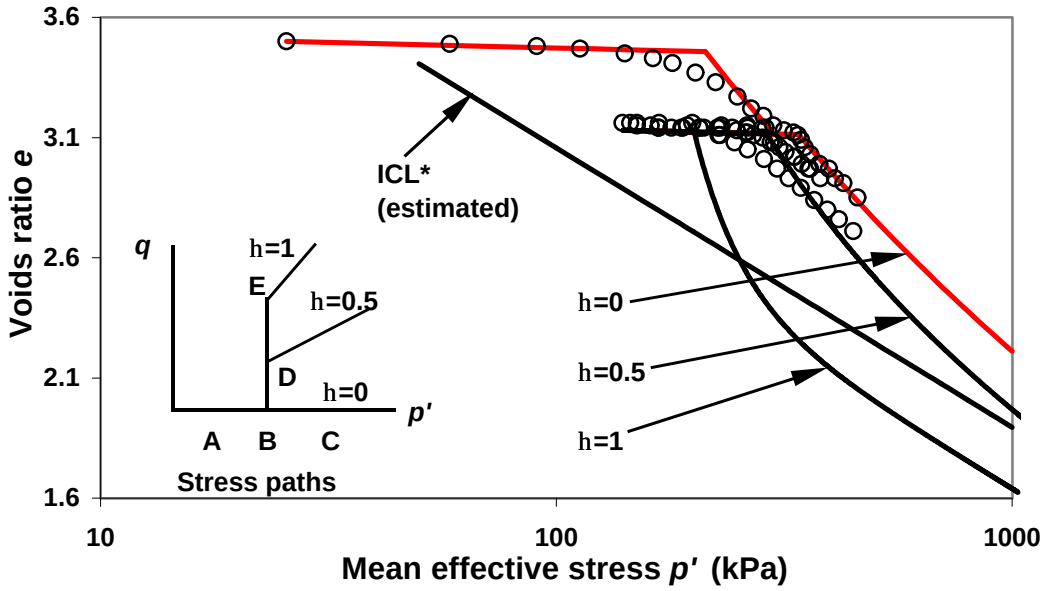

Fig. 14 Compression behaviour of an artificially cemented clay (Test data after Burghignoli *et al* , 1998)

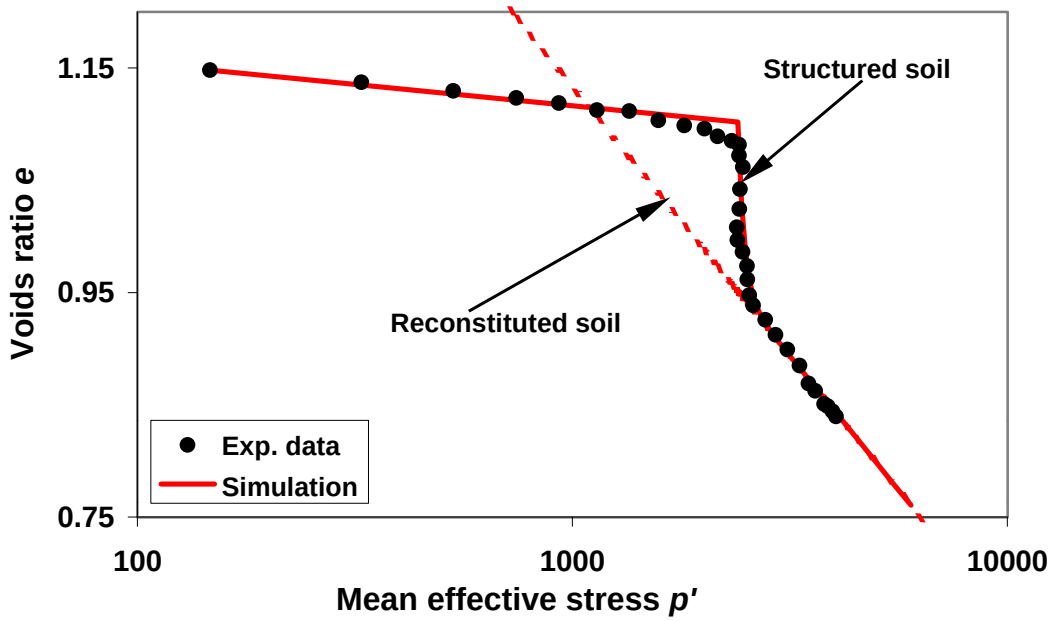

Fig. 15 Isotropic compression test on a calcarenite (Test data after Lagioia and Nova, 1995)

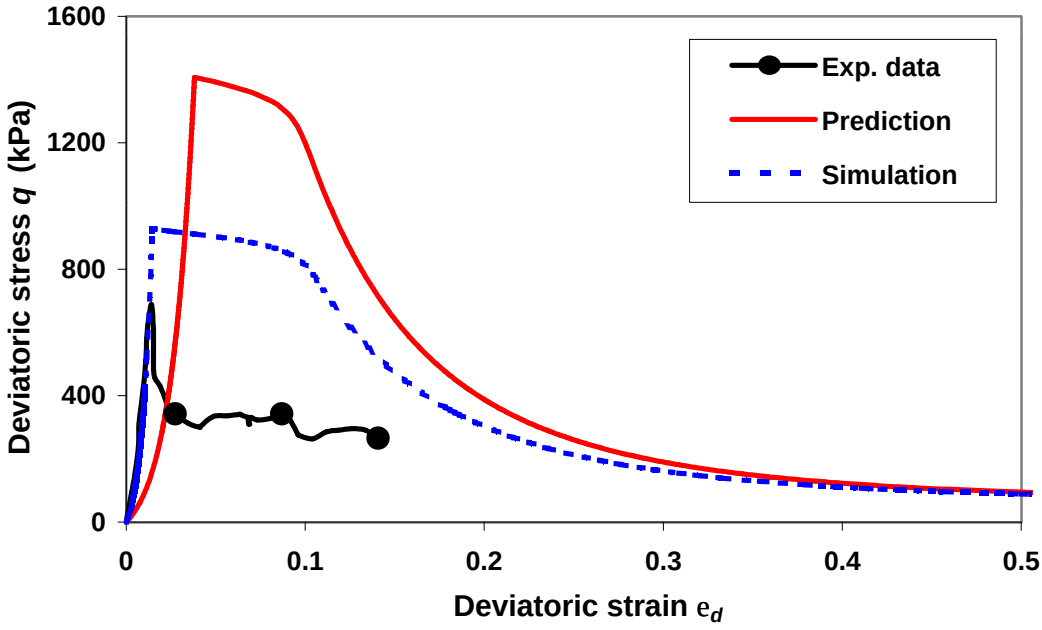

(a) Deviatoric stress and strain relationship

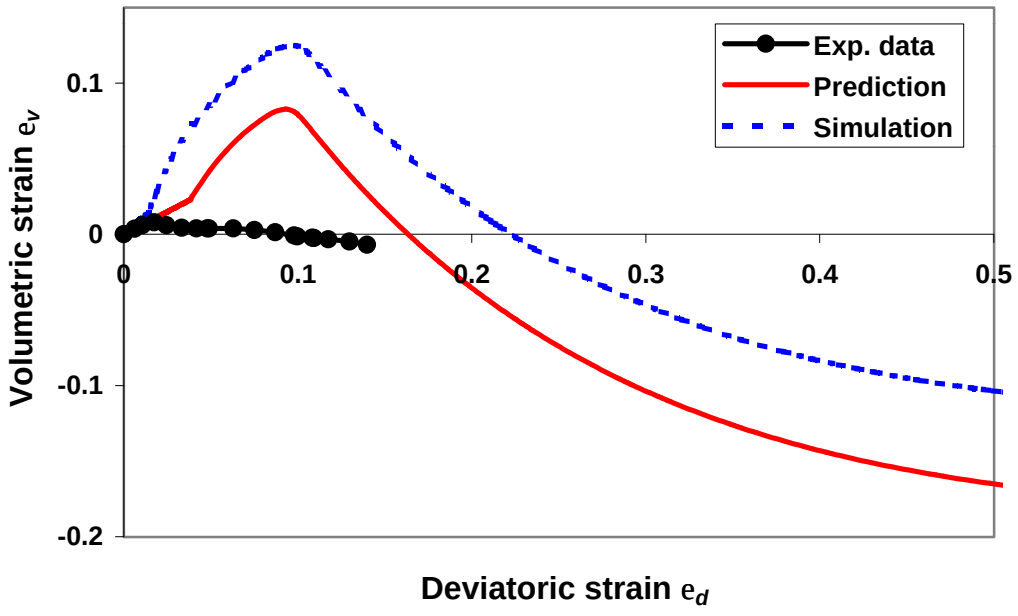

(b) Volumetric strain and deviatoric strain relationship

Fig. 16 Shearing behaviour of a calcarenite at σ'_3= 25 kPa (Test data after Lagioia and Nova, 1995)

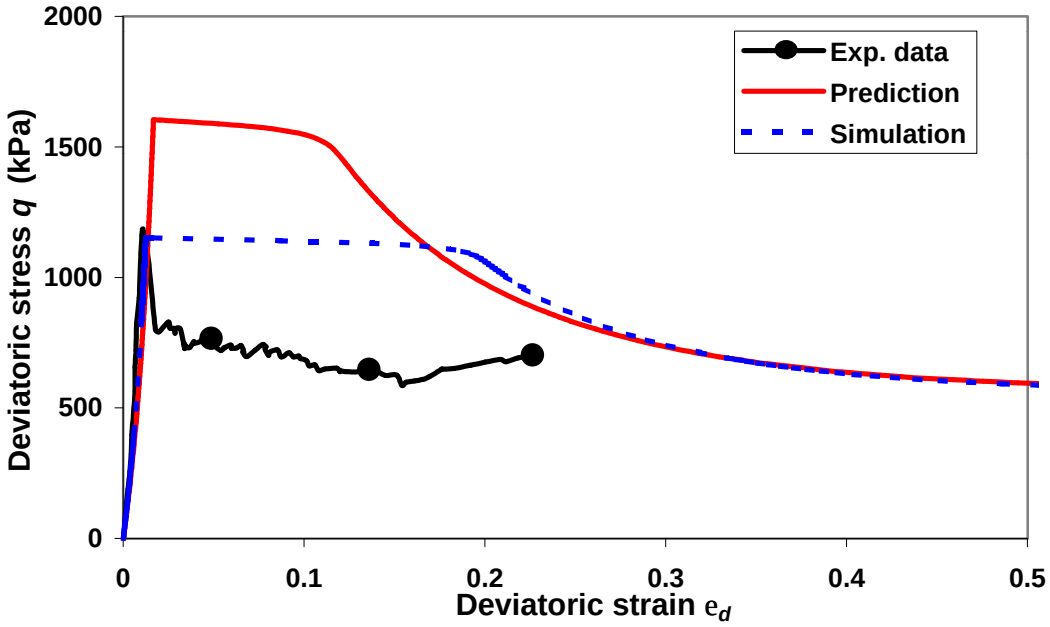

(a) Deviatoric stress and strain relationship

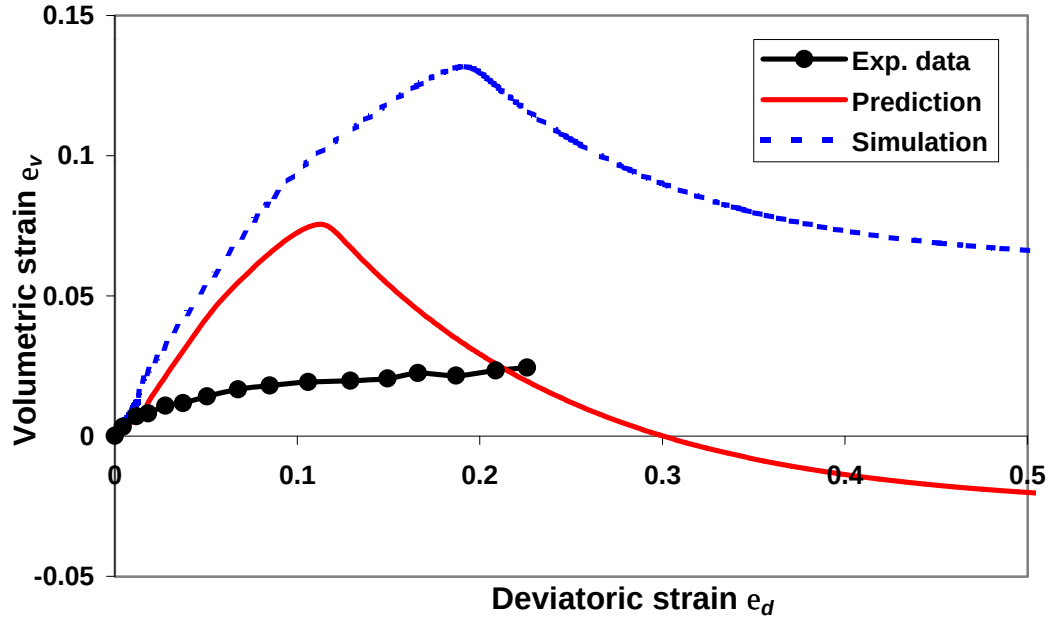

(b) Volumetric strain and deviatoric strain relationship

Fig. 17 Shearing behaviour of a calcarenite at s'_3= 200 kPa (Test data after Lagioia and Nova, 1995)

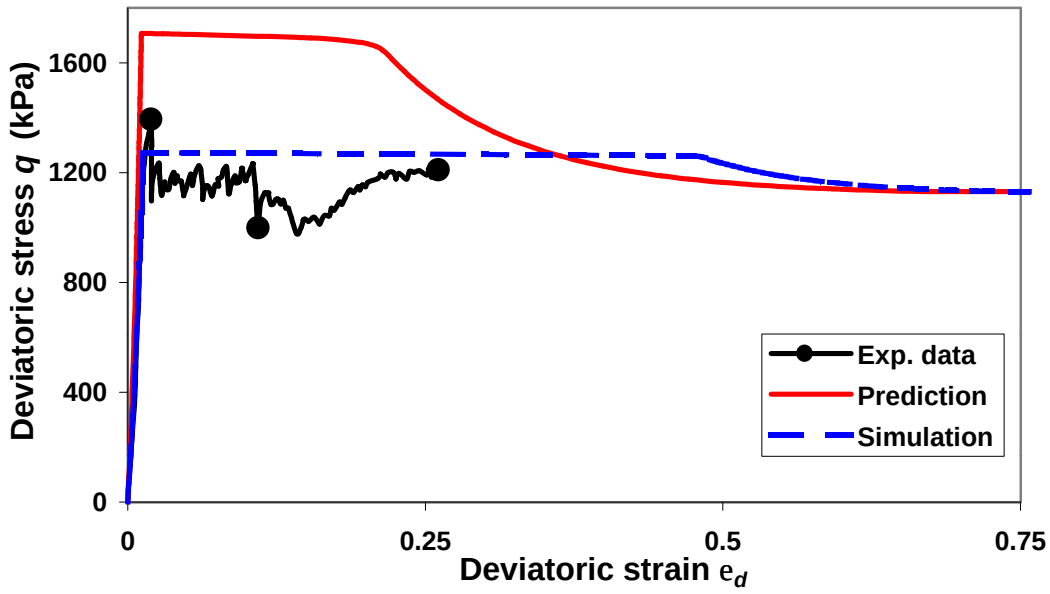

(a) Deviatoric stress and strain relationship

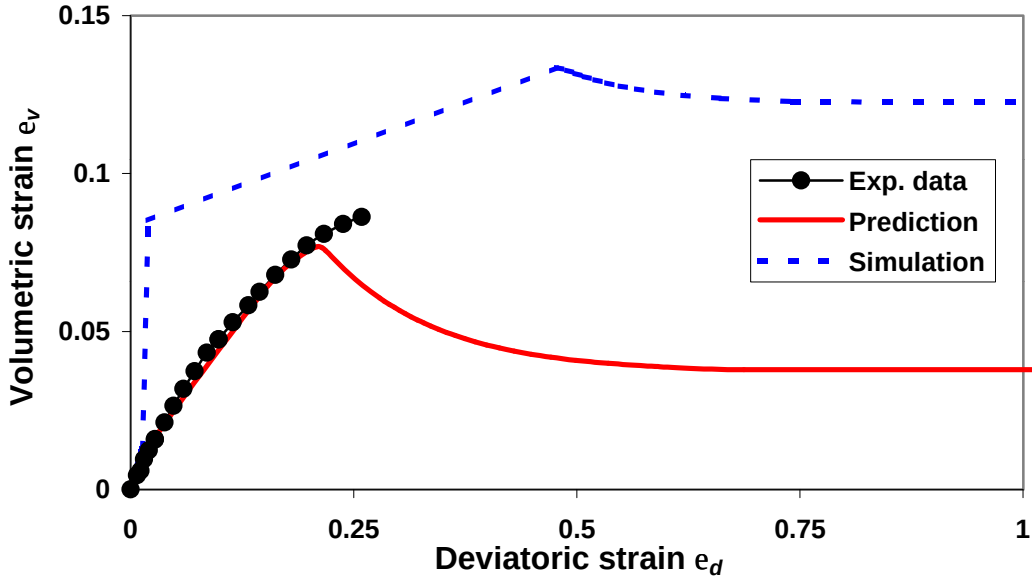

(b) Volumetric strain and deviatoric strain relationship

Fig. 18 Shearing behaviour of a calcarenite at s'_3= 400 kPa (Test data after Lagioia and Nova, 1995)

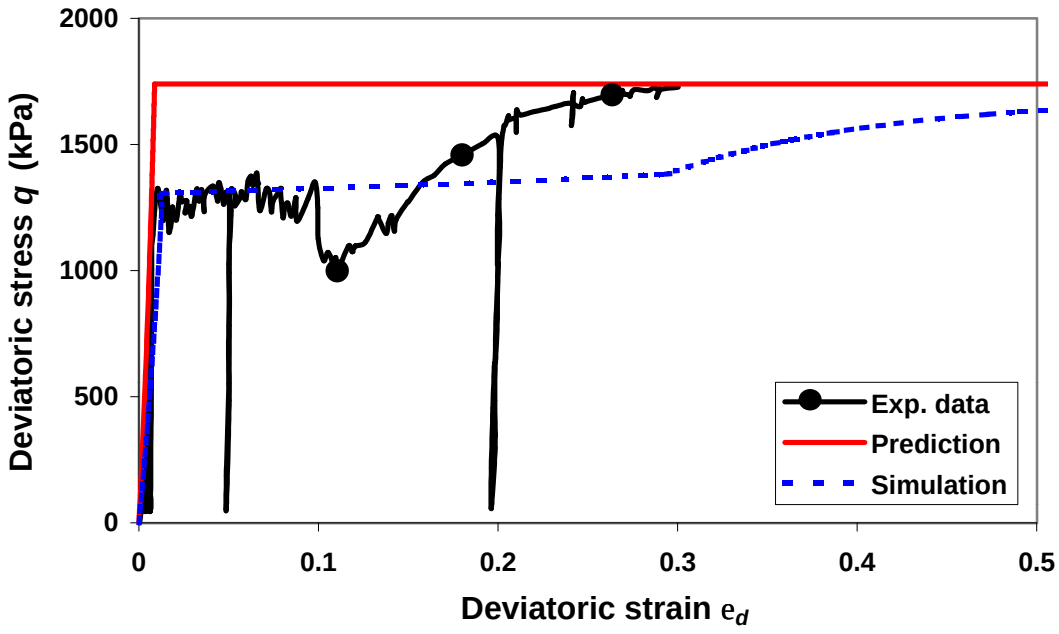

(a) Deviatoric stress and strain relationship

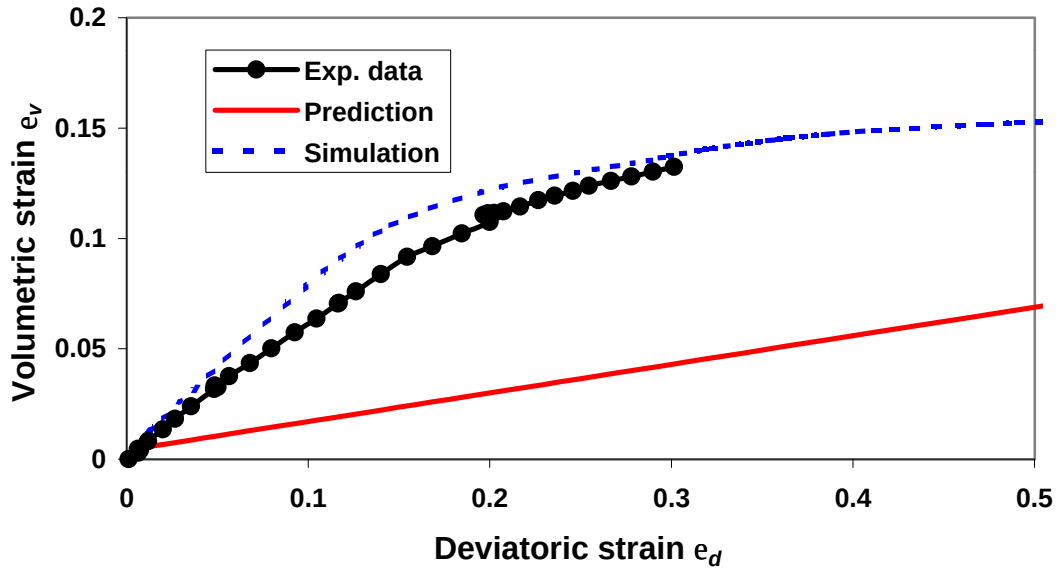

(b) Volumetric strain and deviatoric strain relationship

Fig. 19 Shearing behaviour of a calcarenite at s'_3= 600 kPa (Test data after Lagioia and Nova, 1995)

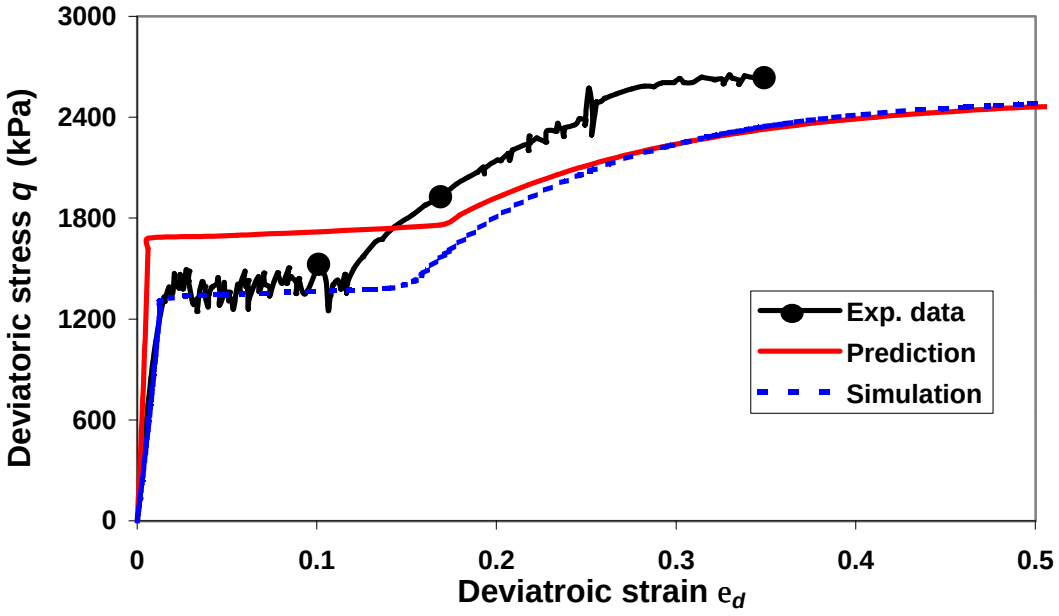

(a) Deviatoric stress and strain relationship

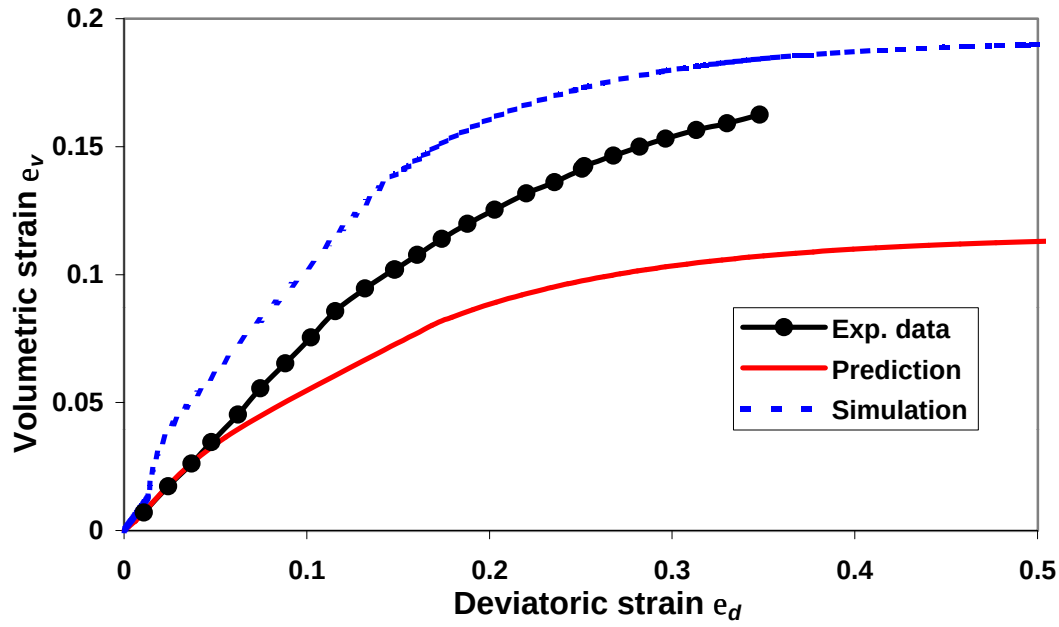

(b) Volumetric strain and deviatoric strain relationship

Fig. 20 Shearing behaviour of a calcarenite at s'_3= 900 kPa (Test data after Lagioia and Nova, 1995)

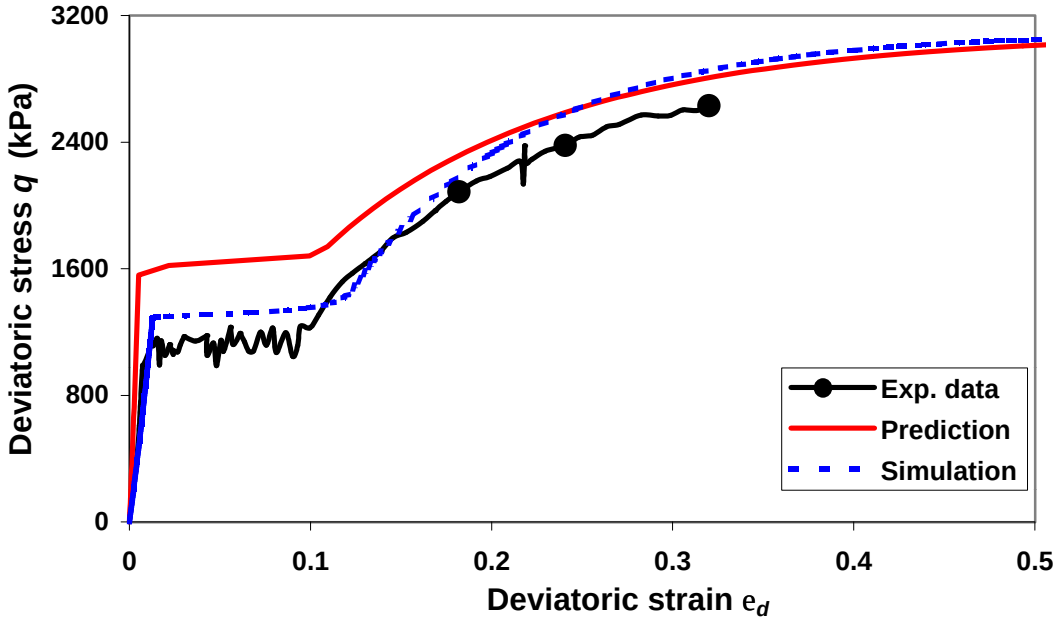

(a) Deviatoric stress and strain relationship

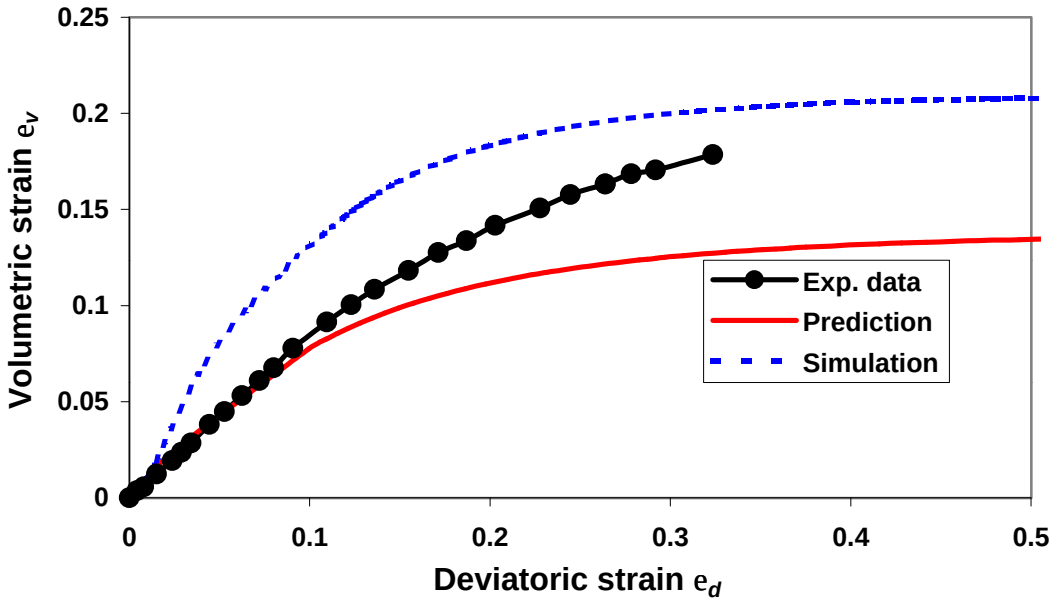

(b) Volumetric strain and deviatoric strain relationship

Fig. 21 Shearing behaviour of a calcarenite at s'_3= 1100 kPa (Test data after Lagioia and Nova, 1995)

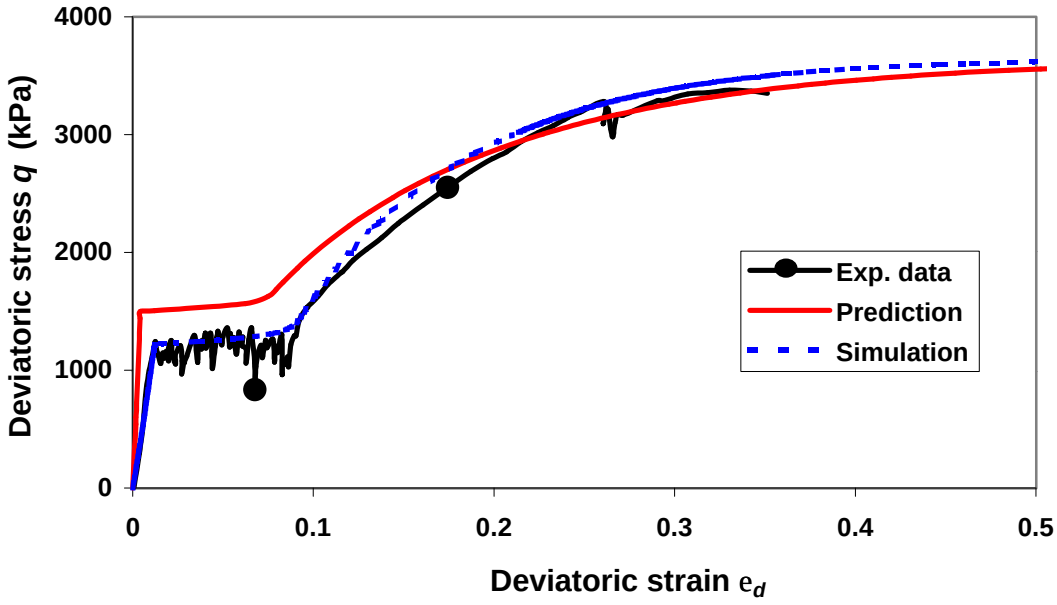

(a) Deviatoric stress and strain relationship

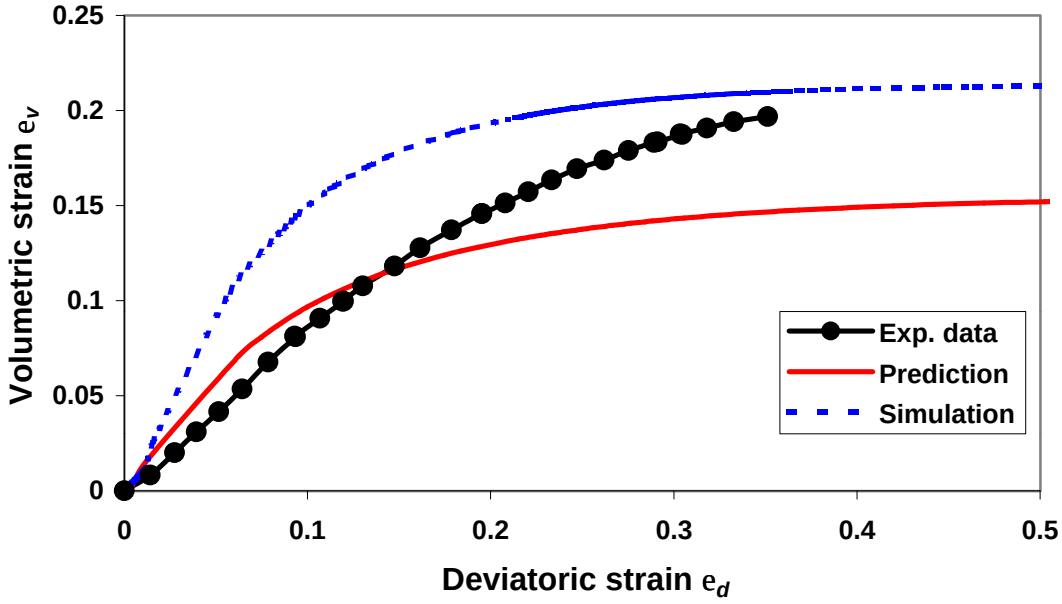

(b) Volumetric strain and deviatoric strain relationship

Fig. 22 Shearing behaviour of a calcarenite at s'_3= 1300 kPa (Test data after Lagioia and Nova, 1995)

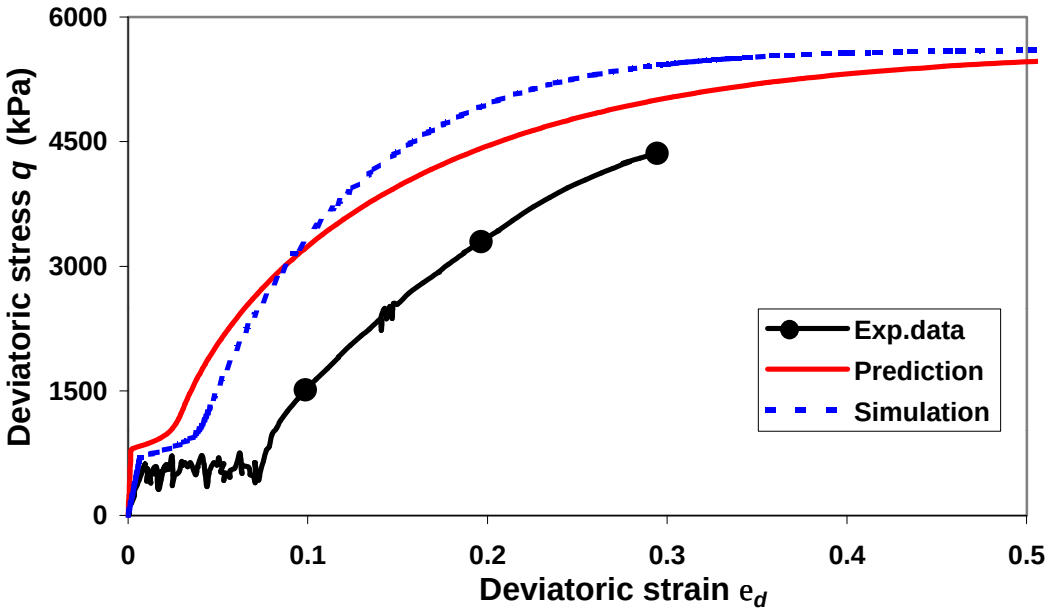

(a) Deviatoric stress and strain relationship

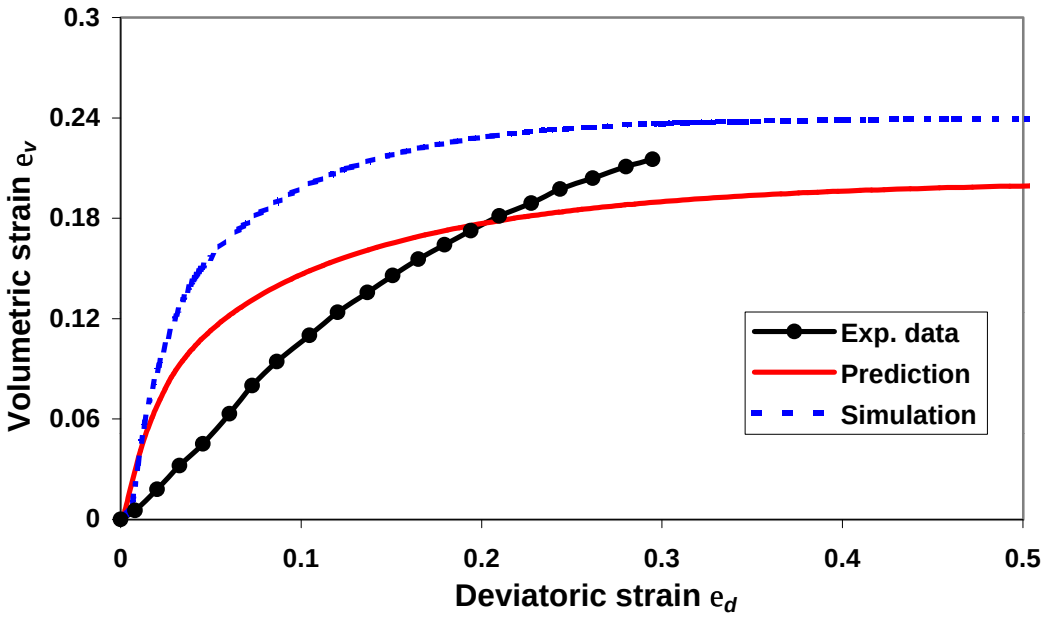

(b) Volumetric strain and deviatoric strain relationship

Fig. 23 Shearing behaviour of a calcarenite at σ'_3= 2000 kPa (Test data after Lagioia and Nova, 1995)

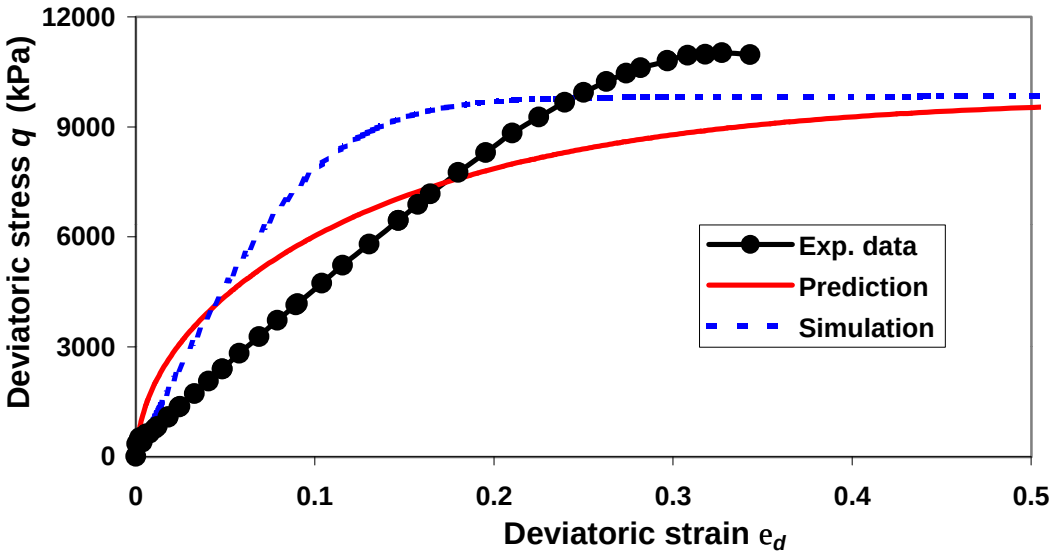

(a) Deviatoric stress and strain relationship

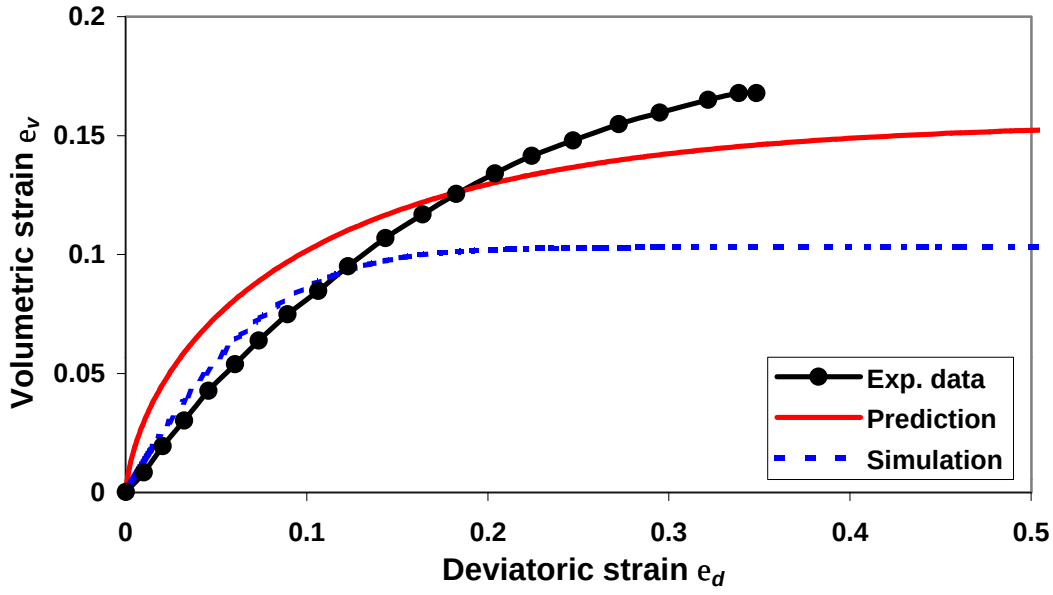

(b) Volumetric strain and deviatoric strain relationship

Fig. 24 Shearing behaviour of a calcarenite at s'_3= 3500 kPa (Test data after Lagioia and Nova, 1995)

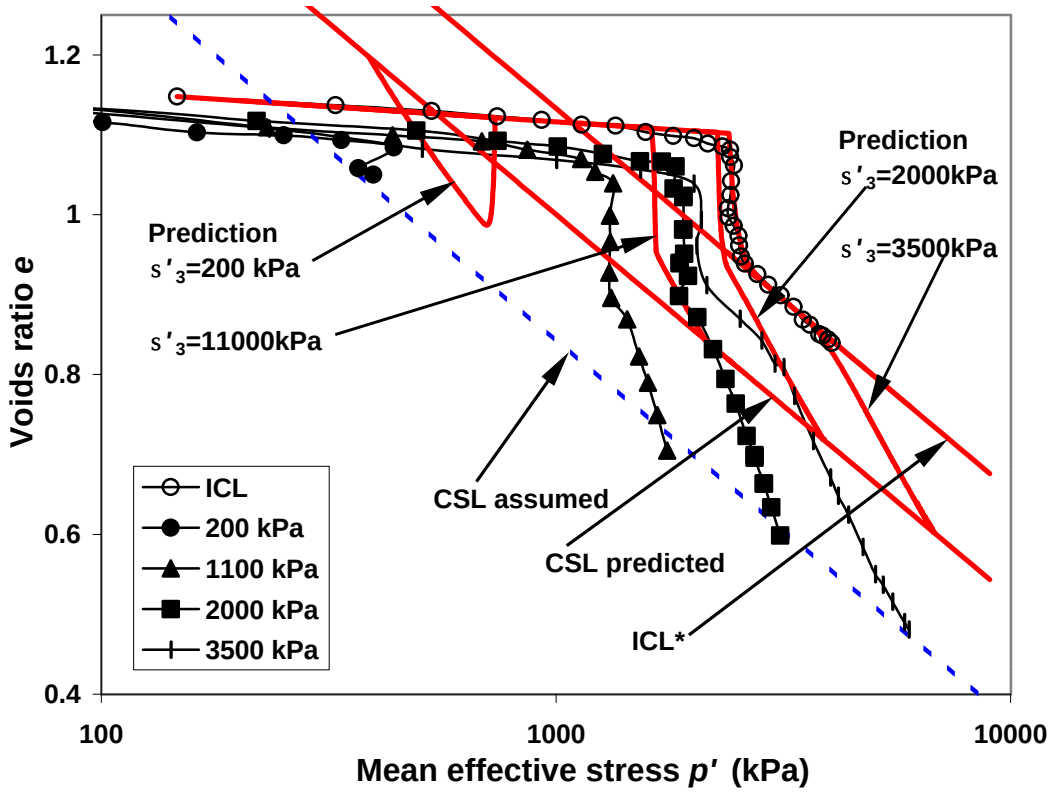

Fig. 25 Stress paths in the *e*-ln*p′* space for tests on a natural calcarenite (Test data after Lagioia and Nova, 1995)

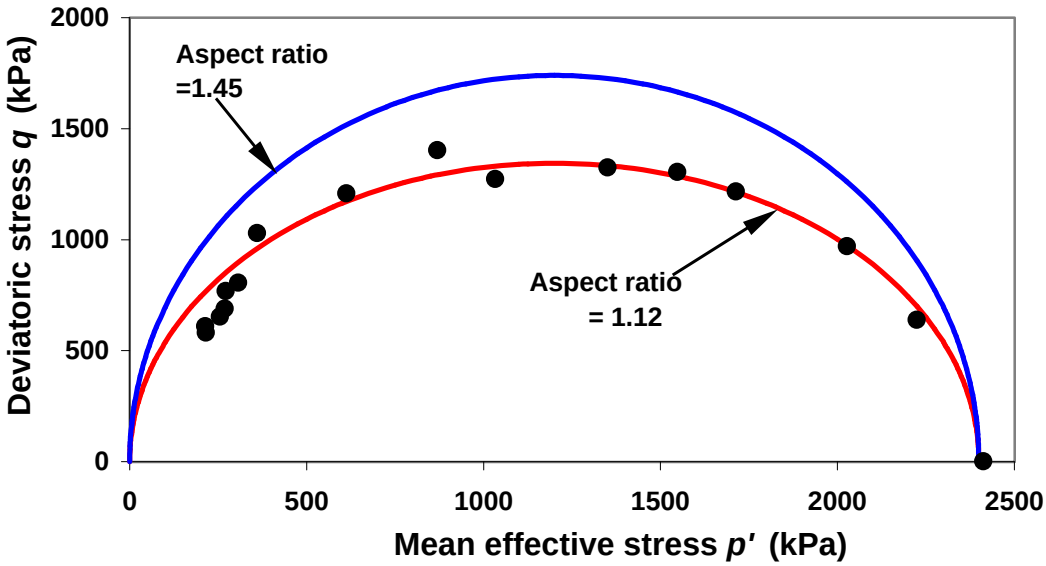

Fig. 26 The initial yield points for a natural calcarenite (Test data after Lagioia and Nova, 1995)

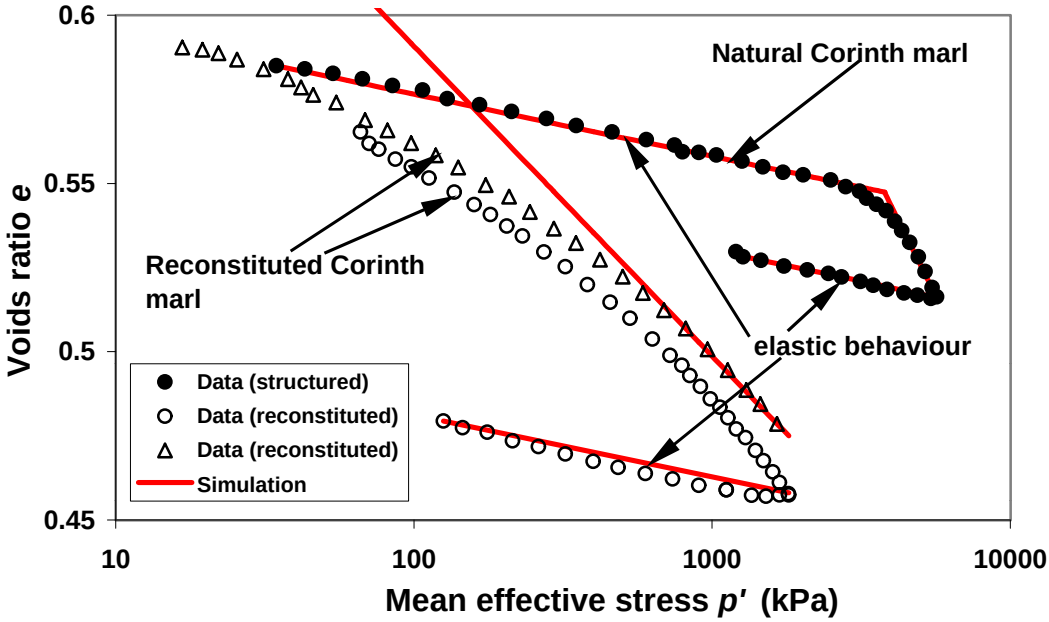

Fig. 27 Isotropic compression behaviour of Corinth marl (Test data after Anagnostopoulos *et al* , 1991)

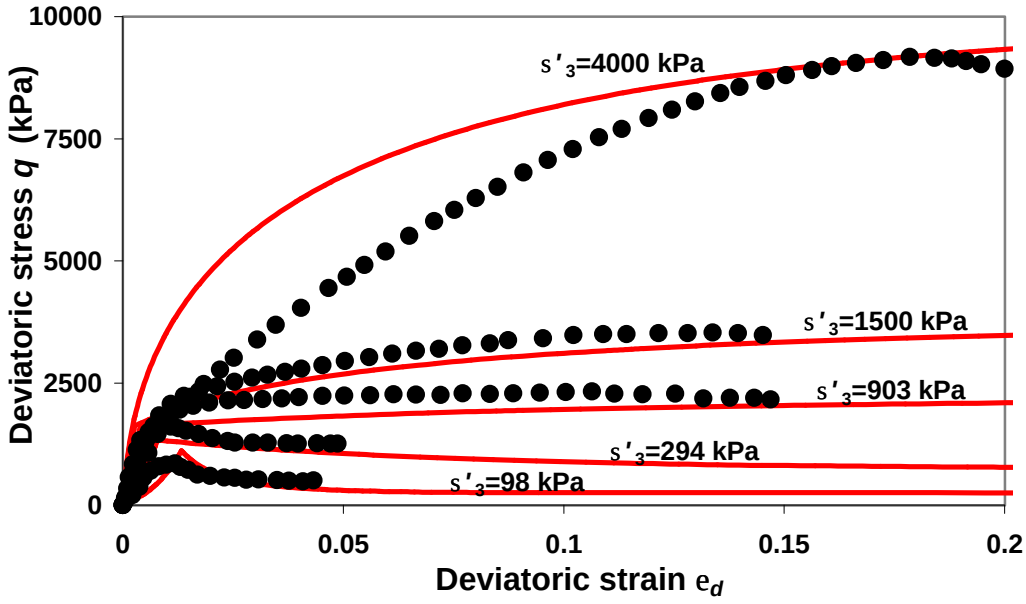

(a) Deviatoric stress and strain relationship

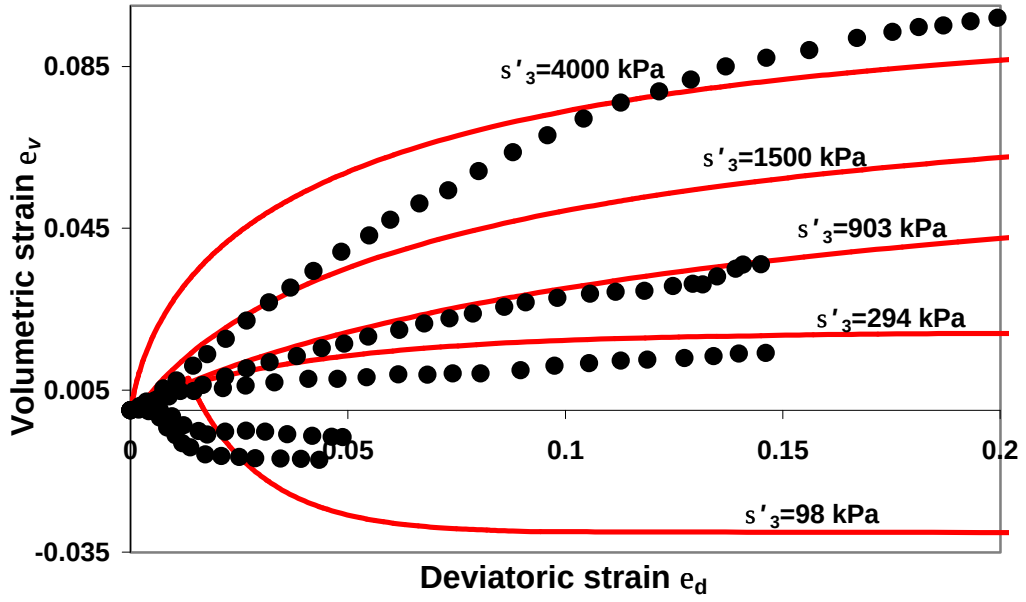

(b) Volumetric and deviatoric strain relationship

Fig. 28 Behaviour of natural Corinth marl (Test data after Anagnostopoulos *et al* , 1991)

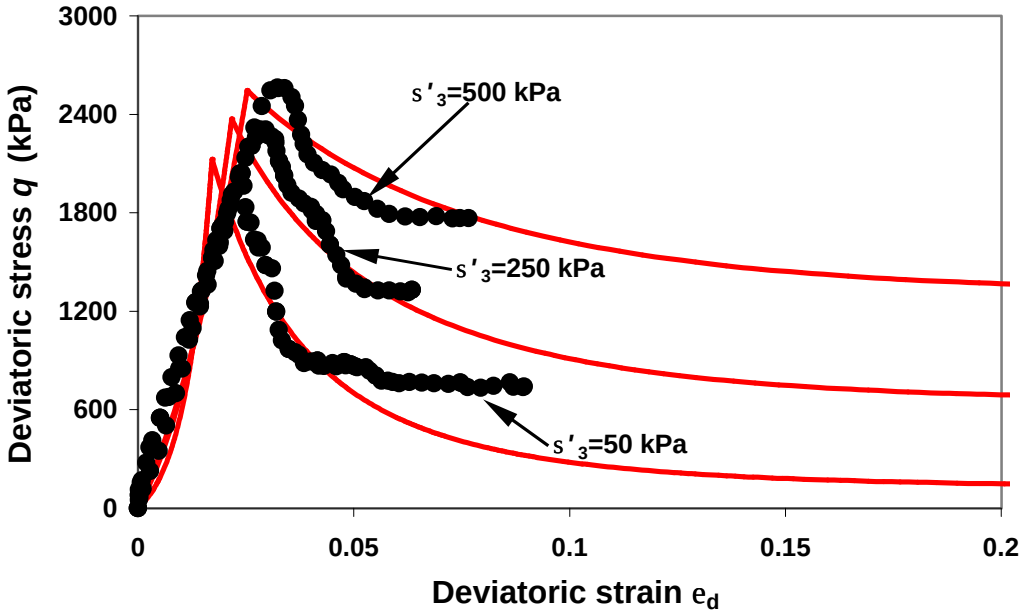

(a) Deviatoric stress and strain relationship

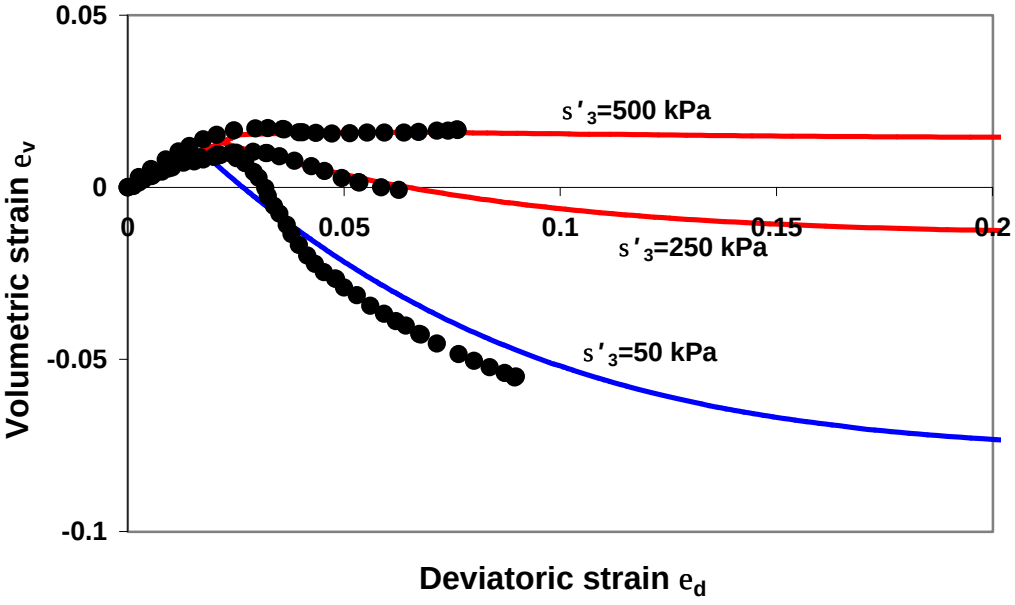

(b) Volumetric strain and deviatoric strain relationship

Fig. 29 Shearing behaviour of a clayshale (Test data after Wong, 1980)